

**Forschungszentrum Karlsruhe**

Technik und Umwelt

Wissenschaftliche Berichte

FZKA 6663

ITER-TA: G 81 TD 05 FE (D452-EU) – Subtask 3

Final Report

EFDA: TW0-SEA3.5/D4

**Three-Dimensional Analysis  
of Combustible Mixture Generation  
in an ITER-FEAT  
First-Wall Coolant Leak Scenario**

W. Baumann, W. Breitung, B. Kaup, G. Necker, P. Royl, J.R. Travis

Institut für Kern- und Energietechnik

Programm Kernfusion

Forschungszentrum Karlsruhe GmbH, Karlsruhe

2001

**Impressum der Print-Ausgabe:**

**Als Manuskript gedruckt  
Für diesen Bericht behalten wir uns alle Rechte vor**

**Forschungszentrum Karlsruhe GmbH  
Postfach 3640, 76021 Karlsruhe**

**Mitglied der Hermann von Helmholtz-Gemeinschaft  
Deutscher Forschungszentren (HGF)**

**ISSN 0947-8620**

**Three-Dimensional Analysis  
of Combustible Mixture Generation  
in an ITER-FEAT  
First-Wall Coolant Leak Scenario**

W. Baumann, W. Breitung, B. Kaup, G. Necker, P. Roysl, J.R. Travis

**Abstract**

Three-dimensional distribution calculations are performed for the ITER-FEAT vacuum vessel, the connected pressure suppression pool and drain tank. An ex-vessel/first-wall coolant leak without plasma shutdown is simulated. The steam, hydrogen, and air sources for this sequence are taken from best-estimate MELCOR calculations. The time- and space-dependent gas distribution in the system is calculated using the verified three-dimensional Computational Fluid Dynamics code GASFLOW. A new extended version of GASFLOW has been developed to model the ITER-FEAT specific phenomena in adequate detail.

During the accident sequence, hydrogen initially appears only in the vacuum vessel due to the steam/beryllium reaction. After failure of the burst membranes, steam and hydrogen flow from the vacuum vessel through the connecting lines to the suppression pool and the drain tank. Because of the ongoing steam condensation occurring in the suppression pool, the pressure there remains permanently at a lower level compared to the other components, resulting in a continuous flow of steam and noncondensable gases into this volume. Since no steam condensation is modeled in the drain tank, almost all H<sub>2</sub> and N<sub>2</sub> accumulate in the suppression pool cover gas volume.

After 10,500 s of steam flow, also air starts entering the vacuum vessel, with the basic mechanisms remaining the same. Consequently, an accumulation of N<sub>2</sub> and O<sub>2</sub> takes place in the suppression pool cover gas. Combustible and explosive H<sub>2</sub>-O<sub>2</sub>-N<sub>2</sub> mixtures exist after 13,600 s, and at 21,000 s a stoichiometric H<sub>2</sub>/O<sub>2</sub> ratio has formed, involving 14 kg of hydrogen.

Contrary to the situation in the suppression pool with its significant hydrogen risk, only inert, steam dominated mixtures without hazard potential develop in the vacuum vessel and the drain tank. Various passive mitigation measures could be considered to reduce or completely remove the hydrogen risk in the suppression pool.

**Dreidimensionale Analyse  
zur Entstehung eines brennbaren Gasgemisches  
bei einem ITER-FEAT Unfallszenario  
mit Leck in der Ersten Wand**

W. Baumann, W. Breitung, B. Kaup, G. Necker, P. Roysl, J.R. Travis

## **Zusammenfassung**

Für den ITER-FEAT Vakuumbehälter und den damit verbundenen Druckabbau- und Drainage-Tank wurden dreidimensionale Verteilungsrechnungen durchgeführt. Dabei wird ein externes Kühlmittleck in der Ersten Wand ohne Plasma-Zusammenbruch simuliert. Die Quellterme zum Unfallablauf für Dampf, Wasserstoff und Luft stammen aus "best-estimate" MELCOR-Rechnungen. Die Gasverteilung im System wird raum- und zeitabhängig mit dem überprüften CFD-Code GASFLOW berechnet. Um spezifische Prozesse bei ITER-FEAT Unfallszenarien in angemessenem Detail modellieren zu können, wurde eine neue erweiterte GASFLOW-Version entwickelt.

Wasserstoff tritt zu Beginn des Unfallablaufes nur im Vakuumbehälter aufgrund der Dampf/Beryllium-Reaktion auf. Nach dem Versagen der Berstscheiben strömen Dampf und Wasserstoff vom Vakuumbehälter durch die Verbindungsrohre in den Druckabbau- und den Drainage-Tank. Durch die Kondensation des Dampfes in der Wasservorlage des Druckabbau-Tanks bleibt der Druck dort stets niedriger als in den übrigen Systemkomponenten, was eine kontinuierliche Strömung von Dampf und nichtkondensierbaren Gasen in diesen Behälter bewirkt. Da im Drainage-Tank keine Dampfkondensation modelliert wird, reichern sich auf diese Weise die nichtkondensierbaren Gase fortlaufend im Gasvolumen des Druckabbau-Tanks an.

Nach 10,500 s kommt zur Dampfströmung unter Beibehaltung der grundlegenden Ablaufmechanismen noch der Lufteinbruch in den Vakuumbehälter hinzu. Dies führt zu einer Ansammlung von Stickstoff und Sauerstoff im Gasvolumen des Druckabbau-Tanks. Ab 13,600 s existiert ein brennbares und explosives  $H_2$ - $O_2$ - $N_2$ -Gemisch. Nach 21,000 s hat sich ein stöchiometrisches  $H_2/O_2$ -Verhältnis mit einer Gesamtmenge von 14 kg Wasserstoff gebildet.

Im Gegensatz zur Situation im Druckabbau-Tank mit seinem erheblichen Wasserstoffrisiko entstehen im Vakuumbehälter und im Drainagetank nur inerte, überwiegend dampfhaltige Gemische ohne Gefährdungspotential. Verschiedene passive Gegenmaßnahmen könnten untersucht werden, um das Risiko im Druckabbau-Tank zu reduzieren oder ganz zu beseitigen.

## LIST OF CONTENTS

1	Introduction and Objectives .....	1
2	Accident Scenario .....	1
2.1	Basics .....	1
2.2	Initial Conditions .....	2
2.3	Sources.....	2
3	GASFLOW Model.....	3
3.1	Short Description of GASFLOW Code.....	3
3.2	GASFLOW Extensions for ITER-FEAT .....	4
3.2.1	Introduction .....	4
3.2.2	Model Development.....	4
3.3	Geometry .....	6
4	Discussion of Results .....	7
4.1	Hydrogen Production Phase.....	8
4.1.1	Pressure, Temperature and Gas Composition .....	8
4.1.2	3d Flow Field .....	9
4.1.3	Spatial Hydrogen Distribution .....	9
4.2	Pure-Steam Inflow Phase .....	10
4.3	Air Ingress Phase .....	10
5	Summary and Conclusions .....	11
	Acknowledgement.....	12
6	References .....	13
7	Appendix: GASFLOW 2.2 Input .....	15
7.1	Hydrogen Production Rate .....	15
7.2	Time-Dependent Functions .....	15
7.3	Input File .....	16
	Figures .....	23



## Executive Summary

The objective of this work is to investigate the formation of combustible hydrogen-air-steam mixtures in the ITER-FEAT for a detailed specified accident sequence with special emphasis on size, location, composition, and hazard potential of the evolving reactive cloud. The results can be used to study the feasibility of risk reducing counter measures.

Three-dimensional distribution calculations are performed for the ITER-FEAT vacuum vessel, the connected pressure suppression pool and drain tank. An ex-vessel/first-wall coolant leak without plasma shutdown is simulated. The steam, hydrogen, and air sources for this sequence are taken from best-estimate MELCOR calculations. The time- and space-dependent gas distribution in the system is calculated using the verified 3d Computational Fluid Dynamics (CFD) code GASFLOW. A new extended version of GASFLOW has been developed to model the ITER-FEAT specific phenomena in adequate detail. In the investigated accident sequence, three distinct phases can be observed: The initial hydrogen generation phase (0 - 5,000 s), the pure-steam injection phase (5,000 - 10,500 s), and the air ingress phase (> 10,500 s). The following results are obtained with respect to pressure, temperature and composition of the gases in the three interconnected vessels.

Hydrogen initially appears only in the vacuum vessel due to the steam/beryllium reaction. After failure of the burst membranes, steam and hydrogen flow from the vacuum vessel through the connecting lines to the suppression pool and the drain tank. Since the steam entering the suppression pool is assumed to condense completely, the noncondensable gases  $H_2$  and  $N_2$  accumulate continuously in the cover gas phase of the suppression pool. No steam condensation is modeled in the drain tank. At the end of the hydrogen generation phase, almost all  $H_2$  and  $N_2$  are found in the suppression pool cover gas. The vacuum vessel and the drain tank are predominantly filled with steam. Due to the continuous vortex and turbulence generation, the gas in each vessel is quite well mixed.

During the second phase, steam continues to enter the vacuum vessel, but the structural temperatures are too low to produce further hydrogen. The concentration of the noncondensable gases  $H_2$  and  $N_2$  has reached such a low level in the vacuum vessel that the still continued "pumping" by steam condensation in the suppression pool does not significantly increase the gas concentration in the suppression pool cover gas. Steam remains the dominant gas component in the vacuum vessel and the drain tank.

The third phase of the accident is characterized by air ingress into the vacuum vessel. The basic mechanisms remain the same, leading to an accumulation of  $N_2$  and  $O_2$  in the suppression pool cover gas. Combustible and explosive  $H_2$ - $O_2$ - $N_2$  mixtures exist after 13,600 s. At 21,000 s a stoichiometric  $H_2/O_2$  ratio has formed, involving 14 kg of hydrogen. Since the gas mixture in the suppression pool evolves from the hydrogen-rich side, flammability and detonability are obtained nearly at the same time, and they persist for many hours. In case of ignition, the transient peak detonation pressure in the suppression pool would reach about 8.8 bar, and the quasi-static pressure after combustion would amount to about 4.4 bar.

The substantial hydrogen risk in the analyzed scenario is restricted to the suppression pool only. Various passive mitigation measures could be considered to control this risk by design optimizations.



# 1 Introduction and Objectives

To better define and justify in-vessel hydrogen limits for the ITER-FEAT safety assessment and licensing process, three-dimensional hydrogen distribution, deflagration and / or detonation calculations are necessary for a variety of accident sequences.

The first investigated scenario assumed air ingress, production of 5 kg hydrogen, formation of a (conservative) stoichiometric hydrogen-air mixture, and ignition of a local detonation [1]. Local pressure loads and impulses to the complex 3d vacuum vessel structure have been determined.

The calculations described in this report represent several advancements in terms of modeling complexity and detail:

1. A mechanistic accident scenario was selected, namely an ex-vessel / first-wall coolant leak without plasma shutdown, which is one of the leading sequences with respect to the hydrogen generation potential;
2. The best-estimate steam, hydrogen and air sources for this sequence (MELCOR calculation) were used as input to GASFLOW;
3. Not only the vacuum vessel (VV), but the combined system including the pressure suppression pool (SP) and the drain tank (DT) was modeled; and
4. The time-dependent and three-dimensional gas distribution in the system was deterministically computed.

The objective of this work is to investigate the formation of combustible hydrogen-air-steam mixtures in the system for a detailed accident sequence with special emphasis on size, location, composition and hazard potential of the evolving reactive cloud. The results can be used to investigate the feasibility of risk reducing counter measures.

## 2 Accident Scenario

### 2.1 Basics

The ex-vessel LOCA scenario leading to an in-vessel release of steam and air was selected for the analysis, because it is one of the most challenging accident sequences for the ITER safety systems [2].

It is assumed that a break in the heat transfer system occurs in the TCWS<sup>\*)</sup> vault without

---

<sup>\*)</sup> Tokamac Cooling Water System

plasma shut-down (Figure 1). The cooling of the affected first-wall section (one loop out of three) is drastically reduced, leading to structural failure of the first wall and an in-vessel breach within a few minutes. Steam from the cooling system is transported through the cooling pipe and the leak into the VV, where it can contact hot beryllium. Sensitivity studies concerning the total hydrogen generation from the steam-beryllium-reaction for the 1995 ITER interim design resulted in up to 67 kg of hydrogen [2]. More refined recent MELCOR calculations for ITER-FEAT gave about 15 kg H<sub>2</sub> [3]:

After the steam inventory in the cooling pipe has been injected into the VV, air enters through the leak as long as the vessel is at sub-atmospheric pressure.

The burst membranes isolating the SP and the DT from the VV open when the differential pressure exceeds 0.8 bar [4].

## 2.2 Initial Conditions

The initial conditions of the gas and structures are summarized in Table 2.1. One third of the torus, corresponding to the failed cooling loop, is assumed to be at a temperature of 1,273 K. The remainder is assumed to have a temperature of 503 K.

The pipes are at 303 K. The internal pressure in the different pipe sections on either side of the burst membranes corresponds to the vessel to which they are connected.

Table 2.1: Initial conditions of the GASFLOW computations.

Parameter	Vacuum vessel	Pressure suppression system	Drain tank
<ul style="list-style-type: none"> <li>• Atmosphere</li> <li>- Temperature (K)</li> <li>- Pressure (Pa)</li> <li>- Species</li> <li>- Total mass (kg)</li> </ul>	1/3 at 1,273 2/3 at 503 500 N <sub>2</sub> 3.5	303 4,200 N <sub>2</sub> 56	303 4,200 N <sub>2</sub> 18
<ul style="list-style-type: none"> <li>• Structures</li> <li>- Temperatures (K)</li> </ul>	1/3 (=120°) of torus walls at 1,273, 2/3 (=240°) at 503 K	303	303

## 2.3 Sources

After the break of the first wall due to the lack of cooling, first steam and later air starts flowing into the ITER-FEAT VV. The time of steam flow onset, coinciding with the initiation of hydrogen production in the VV, is taken as the starting point of the GASFLOW simulation. As

all flow rate and temperature information provided by the ITER-JCT contains a large and detailed amount of data covering even several hundred seconds prior to steam flow onset, the original data tables were simplified and shortened in order to obtain a minimum of representative values. Also the time column was shifted to have steam flow onset specified as time = 0 in order to save computing time (Figure 2 - Figure 9).

The GASFLOW code requires all time-dependent input functions to be prepared in a special format, e.g., steam and air flow rates have to be combined into one total mass flow rate (Figure 5), and its components must be specified as mass fractions in additional table columns (Figure 6, Appendix 7.2).

Moreover, according to GASFLOW instructions, all time-dependent input quantities, i.e. total mass flow rate, mass fractions, flow pressure and flow temperature, must refer to the same points in time. Therefore, the data received from the ITER-JCT, after being reduced to a fewer number of values, were interpolated in order to apply one single time scale to all input quantities.

The various curves representing the accumulated masses of steam, nitrogen, and oxygen shown in Figure 2 - Figure 4 were generated by smoothing and integrating the mass flow rates received from the ITER-JCT. In contrast, the hydrogen production rate (Figure 9) was derived from given hydrogen production data (Figure 10) prior to smoothing.

The time-dependent temperature of the steam and air flowing into the VV is depicted in Figure 7 and Figure 8. These MELCOR results were used as input to the GASFLOW calculation.

## **3 GASFLOW Model**

### **3.1 Short Description of GASFLOW Code**

The GASFLOW code has been developed in a cooperation between Los Alamos National Laboratory (LANL) and Forschungszentrum Karlsruhe (FZK) [5], [6]. GASFLOW is a 3d-fluid dynamics field code which is used to analyze 3d-flow phenomena such as circulation patterns; flow stratification; hydrogen distribution mixing and stratification; combustion and flame propagation; effects of noncondensable gas distribution on local condensation and evaporation; and aerosol entrainment, transport, and deposition [7] - [13].

GASFLOW is a finite-volume code based on robust computational fluid dynamics techniques that solve the compressive Navier-Stokes equations for 3d-volumes in Cartesian and cylindrical coordinates. A semi-implicit solver is used to allow large time steps. The code can model geometrically complex facilities with multiple compartments and internal structures, and has transport equations for multiple gas species, liquid water droplets, and total fluid internal energy. A built-in library contains the properties of 23 gas species and liquid water. GASFLOW can simulate the effects of two-phase dynamics with the homogeneous equilib-

rium model, two-phase heat transfer to and from walls and internal structures, catalytic hydrogen recombination and combustion processes, and fluid turbulence.

## 3.2 GASFLOW Extensions for ITER-FEAT

### 3.2.1 Introduction

GASFLOW II has been extended to model the specific conditions for the ITER-FEAT problem. It was necessary to make three code modifications:

1. An isentropic expansion model to introduce super-heated water vapor and air into the plasma chamber;
2. A hydrogen production - steam destruction model to simulate the  $\text{Be} + \text{H}_2\text{O} > \text{BeO} + \text{H}_2$  chemical reaction in fluid cells adjacent to the hot beryllium surfaces; and
3. A water vapor destruction and energy destruction model to simulate the effects of the water pressure suppression pool. These models will be discussed below.

### 3.2.2 Model Development

#### A. Isentropic Expansion Model

It was convenient to develop an analytical expression to pre-expand the steam source (at roughly 1 bar or 100,000 Pa) to the pressure of the plasma chamber, which initially is at 500 Pa, so that exceptionally high velocities can be avoided. We have implemented the expression for a reversible adiabatic process given in any introductory textbook on thermodynamics as

$$\frac{T_2}{T_1} = \left( \frac{P_2}{P_1} \right)^{\frac{\gamma-1}{\gamma}} \quad (3.1)$$

where in our case  $P_1$  is known to be 1 bar (100,000 Pa),  $T_1$  is a time-dependent function known from the source term to start around 1,000 °C (1,273 K) and monotonically decrease over 30,000 s to about 340 °C (613 K), and  $P_2$  can be thought of as a reference pressure in the plasma chamber. From Eq. (3.1), given the ratio of specific heat capacities  $\gamma$ , we can compute  $T_2$ , which then uniquely defines the fluid density so that correct mass flow rates (also known as a time-dependent quantity) of material can be convected into the plasma chamber. The configuration of the "reservoir", which provides the source of injected material into the plasma chamber is shown in Figure 11 and Figure 12.

The isentropic exponent  $\gamma$  is determined to be 1.28 from the steam tables to correctly calculate an expansion of steam from 100,000 Pa, 1,273 K to 500 Pa, 400 K. GASFLOW makes use of the standard "sortam" file [6] to define the source term in conjunction with the new required input additions: The 10<sup>th</sup> location of the `gasdef` statement now has the capability to specify the analytical isentropic expansion given by Eq. (3.1) by inputting either a -401 for

mass fractions or -402 for volume fractions; a packed i,j,k,iblock locator for the reference pressure, **pref**; and an input value for **gamma**. If **pref** is positive, then the reference pressure is a constant rather than the time-dependent value specified by the location of the packed notation. A complete description to specify the source is given here with the XPUT NAMELIST input variables and the sortam file described elsewhere:

```
; the following input is required for the superheated steam source to
; isentropically expand it to the plasma chamber low pressure
tshift_sortam = 10.0, ; time shift the sortam file by 10s
sortami = 2,
holes(1:13,37) = 15, 16, 13, 14, 10, 11, 1, 1, 0, 0, 0,
0, 0, ; reservoir location
gasdef(1:18,18) = 15, 16, 13, 14, 10, 11, 1, -1,-2, -401, 0.,
999999., 'h2o', -304, 'n2', -305, 'o2', -306,
subsodef(1:7,1) = 15, 16, 13, 14, 10, 11, 1,
zeroddef(1:7,1) = 15, 15, 13, 14, 10, 11, 1,
vbc(1:10,1) = 15, 15, 13, 14, 10, 11, 1, -1, 0.0, 999999.,
vvalue = 0.0,
pref = -17131101, ; i=17, j=13, k=11, iblk=1 reference pressure location
gamma = 1.28, ; ratio of specific heats
```

The reader is referred to the GASFLOW User's manual [6], for additional discussions about the input and sortam source file.

## B. Hydrogen Production Model

A time-dependent hydrogen production table is given in the "H<sub>2</sub>-rate" table (Appendix 7.1). It is understood that this hydrogen source comes from the oxidation of hot beryllium through the chemical equation



where 1/3 of the hydrogen production occurs on the "Inboard" beryllium surfaces and 2/3 occur on the "Outboard" beryllium surfaces. We define those hydrogen production (and steam destruction) computational cells shown in Figure 13 as all those that touch the beryllium surfaces in the 120 degree segment shown in Figure 12.

The mechanics of computing the hydrogen production / steam destruction terms in the mass and energy equations proceeds as follows:

1. The given table for hydrogen production rate (Appendix 7.1) is interpolated for the current simulation time.
2. Steam concentrations are computed for all fluid computational cells touching hot beryllium on both the inboard and outboard locations shown in the 120 degree segment of Figure 12 and the vertical cut through the plasma chamber shown in Figure 13.
3. The summation of the inboard and outboard concentrations is performed so that steam destruction and hydrogen production can be weighted according to steam concentration fractions.
4. The steam mass equation is calculated to reflect this destruction effect, and the energy lost in the energy equation associated with this mass destruction is computed assuming the mass is lost at the local temperature of the fluid itself.

5. The hydrogen mass equation is evaluated to reflect the production effect with mass born at an energy equaling 1,000 °C (1,273 K).

### C. Suppression Pool Model

After the rupture disk fails between the plasma chamber and the pressure suppression pool, steam, hydrogen, nitrogen, and eventually oxygen under a favorable pressure gradient are convected through a pipe connecting the plasma chamber to the pressure suppression pool, containing a total of 400 m<sup>3</sup> of water. This rather large volume of water is held roughly constant at 30 °C (303 K) as the steam is condensed and the noncondensable gases (H<sub>2</sub>, N<sub>2</sub>, and O<sub>2</sub>) are added to the mass and energy inventory of the pressure suppression pool cover gas. The mechanics of this model are as follows:

1. All steam mass and the associated energy are removed from the cover gas as it is assumed that steam condenses in the water pool.
2. Energy for the noncondensable gases is reduced to the temperature of the water pool, which is assumed to be constant at 30 °C (303 K). MELCOR calculations have shown that the water pool temperature remains at this temperature level.

### D. GASFLOW Input for the Hydrogen Production and Suppression Pool Models

We have elected to use our general integer and real variable input, in the XPUT NAMELIST, to specify input variables for these two specialized models for the ITER-FEAT program. The required input with a description follows:

```
$xput
  intinp(1) = 1, ; initialize ITER-FEAT models by calling setupITER
  intinp(2) = 1, ; call h2ITER from burn.f90 to generate h2 & destroy h2o
  intinp(3) = 3, ; block number for destroying h2o (pressure suppression pool)
  intinp(11) = 2, ; ibeg to search for cells touching hot Be
  intinp(12) = 15, ; iend to search for cells touching hot Be
  intinp(13) = 5, ; jbeg to search for cells touching hot Be
  intinp(14) = 23, ; jend to search for cells touching hot Be
  intinp(15) = 2, ; kbeg to search for cells touching hot Be
  intinp(16) = 21, ; kend to search for cells touching hot Be
  intinp(17) = 1, ; block number to search for cells touching hot Be
  intinp(18) = 4, ; i cutoff (> for outboard; otherwise inboard)
  realinp(1) = 1273.000005, ; temperature cutoff to search for cells touching hot Be
  realinp(2) = 303.0, ; gas temperature for suppression pool
  .
  .
```

## 3.3 Geometry

The geometry model used in the GASFLOW calculations is summarized in Figure 14. Under normal operation, the VV is isolated from the DT and the SP by burst membranes in the connecting pipes. The burst membranes are supposed to open when a differential pressure of 0.8 bar is reached.

The main data of the GASFLOW geometry model are summarized in Table 3.1.

Table 3.1: Data of GASFLOW geometry model for ITER-FEAT vessels and connecting pipes.

Property	Vacuum vessel	Press. suppr. pool	Drain tank	Pipes		
				1	2	3
Volume (m <sup>3</sup> )	1,350	1,200	400	0.922	0.922	2.356
Radius (m)	10.0	8.49	5.0	0.225	0.225	0.125
Length (m)				5.8	5.8	48
Elevations (m)						
- upper	+4.3	21.5	-6.0	-4.3	-4.3	21.24
- lower	-4.3	16.2	-11.0	-6.0	-6.0	0.064
Computational grid						
- r,z,θ nodes	20 x 54 x 20	8 x 12 x 10	5 x 12 x 10	1 x 1 x 10	1 x 1 x 10	1 x 1 x 10
- total nodes	21,600	960	600	10	10	10

## 4 Discussion of Results

In view of the quite complex and interacting physical processes in the investigated scenario, it is helpful to subdivide the sequence of events into three phases:

1. Hydrogen production phase,
2. Pure-steam inflow phase, and
3. Air ingress phase.

The first phase covers the time interval during which the beryllium surface of the failed loop is sufficiently hot for a noticeable hydrogen production by the steam-beryllium reaction. This phase lasts about 1 hour.

During the second phase, steam continues to enter the VV, but the structure (beryllium) has cooled to temperatures which allow no significant hydrogen production rates. This situation lasts about two more hours.

The third phase starts about 3 hours after accident initiation. It is characterized by air ingress. After blowing the steam inventory of the cooling pipes into the VV, air break-through occurs from the vault via the in-vessel leak. Without counter measures this phase lasts about one day, until pressure equilibrium is obtained between the outer atmosphere and the three connected ITER vessels.

## 4.1 Hydrogen Production Phase

### 4.1.1 Pressure, Temperature and Gas Composition

After formation of an in-vessel leak, steam of 1,273 K and 1 bar pressure enters the VV. The pressure and temperature development in the VV is quite complex during this initial phase of the accident, because of the time-dependent steam source, the expansion cooling of the steam, the compression heating of the gases from the on-going steam injection, the hydrogen production, steam destruction and the sudden opening of burst membranes.

Figure 15 shows the calculated pressure histories for the VV, the SP and the DT up to 5,000 s. The three burst membranes open simultaneously at about 820 s, allowing strong pressure equilibration flows from the VV to the SP and to the DT. All steam flowing into the SP is assumed to condense, and the observed pressure increase in the SP is due to the accumulation of noncondensable gases ( $H_2$ ,  $N_2$ ). In the DT, no steam condensation is assumed to occur. At 5,000 s the three vessels have reached pressures near 0.2 bar.

Figure 16 summarizes the average temperatures in the three communicating vessels. Prior to the burst membrane rupture the gas temperature in the VV reaches about 1,000 K due to compression heating from the steam injection. The average gas temperature in the SP is fixed in the model to the initial value of 303 K, because the water mass of the pool ( $650 \text{ m}^3$ ) is much larger than the steam mass transported into the SP. In the DT, a maximum gas temperature of about 750 K is predicted.

Figure 17 presents calculated hydrogen masses in the three vessels up to 5,000 s. About 11 kg of the hydrogen have accumulated in the VV up to the time of membrane failure. From there on, the continuing steam condensation in the SP acts as a pump for noncondensable gases. At 5,000 s almost the complete hydrogen which was generated in the VV and partly transported to the DT, has been drawn into the SP (about 14 kg). Only 0.6 kg remain in the DT, and practically no hydrogen is left in the VV by that time.

The same redistribution occurs with nitrogen, which is the other noncondensable gas in the system. At 5,000 s only 0.3 kg  $N_2$  remain in the VV, 7 kg in the DT, but 68 kg of nitrogen are found in the SP gas volume. The atmosphere in the VV and the DT consists mainly of steam.

Table 4.1 summarizes the gas inventories at 5,000 s. The gas separation process will continue as long as steam condenses in the SP.

At the end of the hydrogen generation phase, a surprisingly simple gas distribution exists in the three ITER-FEAT vessels:

- The noncondensable gases hydrogen and nitrogen have accumulated in the SP gas volume; and
- The other two vessels are mainly filled with steam.

Table 4.1: Calculated gas inventories (kg) of the three vessels at the end of the hydrogen production phase (5,000 s).

Vessel	H <sub>2</sub>	N <sub>2</sub>	Steam
- Vacuum vessel	0.03	0.3	135
- Suppression pool (gas volume)	13.8	68	0
- Drain tank	0.6	7	24

#### 4.1.2 3d Flow Field

It is important to note that the above given average values for the gas temperatures, pressures and total masses result from complex 3d flow patterns, which are due to strong asymmetries in the geometrical boundary conditions, the gas sources and sinks, as well as connecting lines between the three vessels. To demonstrate the complicated flow field, some 2-d cuts through the velocity field are presented.

Figure 18 depicts the horizontal cut through the velocity field at the plane of steam injection into the VV ( $t = 5,000$  s). The steam flow is redirected in a complicated way by the inboard blanket and also influenced by the location of the pipe leading to the SP (at 2 o'clock position).

Figure 19 shows a vertical cut through the computed flow velocity field in the VV at the location where the pipe connects into the DT (in lower right corner of computational domain, see Fig. 2.4). Two large vortices exist in the vessel at this location and time.

Figure 20 and Figure 21 demonstrate that also in the DT and the cover gas of the SP large vortices are formed in the flow field. The characteristic mixing time constant  $\tau$ , which may be defined as

$$\tau = \frac{\text{characteristic length of vessel}}{\text{average flow velocity}} = \frac{(\text{Volume})^{1/3}}{\bar{v}} \quad (4.1)$$

is in all three vessels below 100 s, which is much shorter than the steam injection period. Therefore, well mixed conditions can be expected for the major volumes of the three vessels.

#### 4.1.3 Spatial Hydrogen Distribution

Aside from the total amount of hydrogen present in each of the three vessels (Table 4.1), the spatial hydrogen distribution is important to judge the hazard potential, once air ingress has started.

The high degree of homogenization in the SP and the DT reached after the end of the hydrogen generation phase is demonstrated in Figure 22 and Figure 23. These Figures present vertical cuts through the H<sub>2</sub>-concentration field in the form of contour plots. Except for small regions near the entrance of the connecting pipe, the hydrogen concentration is very uniform

in the rest of the volume. The directed gas stream coming from the pipe and entering the vessel creates sufficient turbulence for well mixed conditions.

## 4.2 Pure-Steam Inflow Phase

During this second phase of the accident, only steam enters the VV because the surface temperature of the failed blanket section has decreased to temperatures which are too low for noticeable hydrogen production. The still continuing steam condensation in the SP draws gas from the VV and the DT, leading to further concentration of noncondensable gases ( $H_2$  and  $N_2$ ) in the SP. This phase lasts up to the start of air ingress which begins at 10,500 s. Due to the reduced steam flow, compared to the first phase, average temperature and pressure change only slightly between 5,000 and 10,500 s (roughly - 50 K, + 5 kPa).

The calculated gas inventories in the three vessels at the end of this second phase (10,500 s) are summarized in Table 4.2. Compared to 5,000 s (Table 4.1), the small hydrogen and nitrogen inventories of the VV and the DT have been even further reduced, while the steam mass has increased. Hydrogen is now concentrated almost completely in the SP.

Table 4.2: Calculated gas inventories (kg) of the three vessels at the end of the pure-steam injection phase (10,500 s).

Vessel	$H_2$	$N_2$	Steam
- Vacuum vessel	0.015	0.17	148
- Suppression pool	14.0	72	0
- Drain tank	0.35	4.3	32

## 4.3 Air Ingress Phase

Since hydrogen is almost completely concentrated in the SP, it is sufficient to follow the mixture evolution in this part of the system. As before, steam condenses in the SP, creating directed flows from the VV and the DT towards the SP. The air entering the VV is drawn in the same direction.

Figure 24 summarizes the computed masses and volume fractions of the different gas components in the SP for the complete problem time. Air ingress starts at 10,500 s. The flammability limit of hydrogen-rich  $H_2$ - $O_2$ - $N_2$  mixtures is reached at an oxygen concentration of 5 vol.% [14]. Combustion experiments with rich  $H_2$ - $O_2$  diluent mixtures (e.g.  $H_2$ -air) have shown that their flammability and detonability limits are practically identical on such large scales as of interest here. In the SP, this limit is reached 3,100 s after air ingress starts, and persists for the rest of the calculation. At 21,500 s a stoichiometric  $H_2$ - $O_2$  ratio has formed. The total pressure is about 0.55 bar.

Further air ingress, combined with the still active steam condensation in the SP, will de-

crease the hydrogen concentration continuously, but detonable mixtures will exist for many hours. The persisting turbulence from the directed pipe flow into the SP will keep the gas well mixed.

Table 4.3: Calculated gas inventories (kg) of the three vessels at the end of the calculation (21,000 seconds), pressure about 0.55 bar.

Vessel	H <sub>2</sub>	N <sub>2</sub>	Steam	O <sub>2</sub>
- Vacuum vessel	0.028	150	162	45
- Suppression pool	14	434	0	110
- Drain tank	0.18	28	55	8

## 5 Summary and Conclusions

Three-dimensional distribution calculations were performed for the ITER-FEAT VV, the SP and the DT. An ex-vessel / first-wall coolant leak without plasma shutdown was simulated. The steam, hydrogen and air sources for this sequence were taken from best-estimate MELCOR calculations. The time and space dependent gas distribution in the system was calculated using the verified 3d Computational Fluid Dynamics (CFD) code GASFLOW. A new extended version of GASFLOW was developed to model the ITER-FEAT specific phenomena in adequate detail. The following results were obtained with respect to pressure, temperature and composition of the gases in the three connected vessels.

In the investigated accident sequence three distinct phases can be observed:

- initial hydrogen generation phase (0 – 5,000 s),
- pure-steam injection phase (5,000 – 10,500 s), and
- air ingress phase (> 10,500 s).

Hydrogen initially appears only in the VV. After failure of the burst membranes at 820 s, steam and hydrogen flow from the VV through the connecting lines to the SP and the DT. Since the steam entering the SP is assumed to condense completely, the noncondensable gases H<sub>2</sub> and N<sub>2</sub> accumulate continuously in the cover gas phase of the SP. No steam condensation is modeled in the DT. At the end of the hydrogen generation phase (5,000 s) about 96% of the total H<sub>2</sub> and 90% of the N<sub>2</sub> are found in the SP cover gas volume. The VV and the DT are predominantly filled with steam. Due to the continuous vortex and turbulence generation, the gas in each vessel is quite well mixed. At 5,000 s the communicating vessels are near 0.2 bar. The average gas temperatures in the three vessels differ noticeably (VV: 520 K, SP: 303 K, DT: 600 K).

During the second phase, steam continues to enter the VV, but the structural temperatures

are too low to produce further hydrogen. The still continuing "pumping" by the steam condensation in the SP further concentrates the noncondensable gases  $H_2$  and  $N_2$  in the SP gas volume. Steam remains the dominant gas component in the VV and the DT.

The third phase of the accident is characterized by air ingress into the VV. The basic mechanisms remain the same, leading to accumulation of  $N_2$  and  $O_2$  in the SP cover gas. A well mixed burnable and detonable  $H_2$ - $O_2$ - $N_2$  mixture is reached at approximately 13,600 s. At 21,000 s a stoichiometric  $H_2/O_2$  ratio has formed. The pressure in the three different vessels has increased to about 0.55 bar.

The simulation was stopped at 21,000 s, because the further mixture evolution is obvious. The mixture in the SP will remain well mixed, the pressure will increase continuously, and the  $H_2/O_2$  ratio will decrease in an easily predictable manner. The atmosphere in the VV and in the DT will remain inert.

The main conclusions of the GASFLOW distribution calculation are as follows:

- combustible mixtures develop only in the cover gas phase of the SP,
- since the mixture in the SP evolves from the hydrogen-rich side, flammability and detonability are obtained nearly at the same time, they persist for many hours,
- in case of ignition, the transient peak detonation pressure (Chapman-Jouguet value) would reach about 8.8 bar, the initial quasi-static pressure after combustion would amount to about 4.4 bar (neglecting the slower process of venting to the VV).

The hydrogen risk of the analyzed scenario is solely due to the SP. The following mitigation approaches could be considered:

1. Prevent steam condensation in the SP. The complete and continuous steam condensation in the SP concentrates hydrogen and removes steam as inhibiting gas component. From a hydrogen risk point of view it would be advantageous to remove the water pool from the SP, thereby preventing the hydrogen accumulation and keeping the steam partial pressure high (similar to the current dry DT design).
2. Investigate the feasibility of inerting the SP, e.g. with Halon or other fire suppression gases.
3. Investigate the applicability of catalytic recombiners. In nuclear fission safety, catalytic recombiners have been developed and qualified to remove hydrogen from lean and steam inerted atmospheres. Their application to rich (inert) mixtures seems in principle possible, but would require additional experimental investigations.

## Acknowledgement

The authors gratefully acknowledge technical support by Drs. Werner Gulden, Hans-Werner Bartels, and Leonid Topilski, Max-Planck-Institut für Plasmaphysik, Garching bei München. The technical review and suggestion by our colleague Dr. Jörg Starflinger and the manuscript preparation by Ms. M. Stassen is also appreciated.

## 6 References

- [1] W. Baumann, W. Breitung, B. Kaup, R. Redlinger, J.R. Travis, "ITER-FEAT Accident Analysis on Hydrogen Detonation Using DET3D and GASFLOW", Report FZKA-6584 (Febr. 2001), Forschungszentrum Karlsruhe.
- [2] Michael J. Gaeta and Brad J. Merrill, Hans-Werner Bartels, Carine Rachel Laval, Leonid Topilski, "Short-Term Hydrogen Production Issues for ITER", Fusion Technology, Vol. 32, Aug. 1997.
- [3] MELCOR calculations, ITER-Team Japan, e-mail by H.W. Bartels (25.2.2001, 28.2.2001), and L. Topilski (20.4.2001), ITER-JCT, Garching bei München.
- [4] Safety Analysis Data List-3 (SADL-3), Vers. 2.9, ITER-Server, 6.3.2001, H.W. Bartels, L. Topilski, T. Honda, ITER-JCT, Garching bei München.
- [5] J.R. Travis, J.W. Spore, P. Royl, K.L. Lam, T.L. Wilson, C. Müller, G.A. Necker, B.D. Nichols, R. Redlinger, "GASFLOW: A Computational Fluid Dynamics Code for Gases, Aerosols, and Combustion", Vol. I, Theory and Computational Model, Reports FZKA-5994, LA-13357-M (1998).
- [6] J.W. Spore, J.R. Travis, P. Royl, K.L. Lam, T.L. Wilson, C. Müller, G.A. Necker, B.D. Nichols, "GASFLOW: A Computational Fluid Dynamics Code for Gases, Aerosols, and Combustion", Vol. II, User's Manual, Reports FZKA-5994, LA-13357-M (1998).
- [7] P. Royl, "GASFLOW Analysis of the Phebus FPT0 Containment Thermal Hydraulics", Proc. of the Annual Meeting on Nucl. Technology '95, Kerntechnische Gesellschaft e.V., Deutsches Atomforum e.V., ISSN 0720-9207, Nürnberg, 16.-18. Mai 1995, p. 107.
- [8] P. Royl, C. Müller, J.R. Travis, T. Wilson, "Validation of GASFLOW for Analysis of Steam/Hydrogen Transport and Combustion Processes in Nuclear Reactor Containments", Proc. 13th Conf. On Structural Mechanics in Reactor Technology, August 13-18, 1995, Porto Alegre, RS, Brazil, Vol. I, 211-16, Univ. Fed. do Rio Grande do Sul, 1995.
- [9] P. Royl, J.R. Travis, E.A. Haytcher and H. Wilkening, "Analysis of Mitigating Measures during Steam/Hydrogen Distributions in Nuclear Reactor Containments with the 3D-Field Code GASFLOW", Proc. OECD/NEA CSNI Workshop on the Implementation of Hydrogen Mitigation Techniques, Winnipeg, Canada, May 13-15, 1996, AECL-11762, 129-41.
- [10] W. Breitung, P. Royl, J.R. Travis, H. Wilkening, "Analysen zur Wasserstoff-Verteilung, Rechenprogramm GASFLOW zur Ermittlung der Wasserstoffverteilung in DWR-Anlage", Atomwirtschaft 6, Juni 1996, p. 411-416.

- [11] P. Royl, J.R. Travis, "Simulation of Hydrogen Transport with Mitigation Using the 3D-Field Code GASFLOW", Proc. 2nd Int. Conf. On Advanced Reactor Safety, June 1-4, 1997, Orlando, Florida, Vol. 1, 578-88, La Grange Park, Ill.: ANS; 1997.
- [12] J.R. Travis, G. Necker, P. Royl, "The Theoretical Bases for the GASFLOW-II Nuclear Reactor Safety Containment Code", Proc. of the Annual Meeting on Nucl. Technology '99, Kerntechnische Gesellschaft e.V., Deutsches Atomforum e.V., ISSN 0720-9207, Karlsruhe, 18.-20. Mai 1999, p. 301.
- [13] P. Royl, H. Rochholz, J.R. Travis, G. Necker, W. Breitung, "Three Dimensional Analysis of Steam/Hydrogen Transport with Catalytic Recombiners in Nuclear Reactor Containments Using the Computer Code GASFLOW", 15th Int. Conf. on Structural Mechanics in Reactor Technology, Post-Conf. Seminar on Containment of Nucl. Reactors, Hoam Conv. Center, Seoul, Korea, Aug. 23-24, 1999.
- [14] R.K. Kumar, "Flammability Limits of Hydrogen-Oxygen-Diluent Mixtures", Journal of FIRE SCIENCES, Vol.3, July/August 1985, p. 245.

## 7 Appendix: GASFLOW 2.2 Input

### 7.1 Hydrogen Production Rate

Time (s)	H2-Rate (g/s)	Time (s) orig.
0.0	0.000E-00	500.0
20.0	0.000E-00	520.0
30.0	1.211E+00	530.0
50.0	7.355E+00	550.0
80.0	1.165E+01	580.0
100.0	1.317E+01	600.0
130.0	1.454E+01	630.0
150.0	1.511E+01	650.0
200.0	1.600E+01	700.0
300.0	1.715E+01	800.0
370.0	1.753E+01	870.0
400.0	1.743E+01	900.0
460.0	1.696E+01	960.0
500.0	1.534E+01	1000.0
710.1	9.790E+00	1210.1
800.1	7.977E+00	1300.1
920.0	6.084E+00	1420.0
1010.0	5.040E+00	1510.0
1160.0	3.937E+00	1660.0
1250.0	3.703E+00	1750.0
1490.0	2.510E+00	1990.0
1730.0	1.676E+00	2230.0
1790.0	8.394E-01	2290.0
2000.1	5.130E-01	2500.1
2300.0	3.470E-01	2800.0
2480.1	2.603E-01	2980.1
3000.0	0.000e+00	3500.0
99999.0	0.000e+00	9500.0

### 7.2 Time-Dependent Functions

GF2.2 SORTAM FILE for ITER-FEAT

NCOLS

6

ivvalues ivtypes

0	1	
0	1	
1	1	-1.0
0	1	
0	1	
0	1	

sec	pressure	Kelvin	gps	xfrh2o	xfrn2	xfro2	orig.Time
0.0	1.00E+06	1264.15	0.000	1.000	0.000	0.000	500.0
10.0	1.00E+06	1276.58	0.000	1.000	0.000	0.000	510.0
30.0	1.00E+06	1273.15	250.000	1.000	0.000	0.000	530.0
350.0	1.00E+06	1123.15	340.000	1.000	0.000	0.000	850.0
370.0	1.00E+06	836.92	350.000	1.000	0.000	0.000	870.0
400.0	1.00E+06	793.15	360.000	1.000	0.000	0.000	900.0
500.0	1.00E+06	746.63	355.000	1.000	0.000	0.000	1000.0

1070.0	1.00E+06	688.61	335.000	1.000	0.000	0.000	1570.0
1130.0	1.00E+06	837.93	333.000	1.000	0.000	0.000	1630.0
3000.0	1.00E+06	753.15	270.000	1.000	0.000	0.000	3500.0
4400.0	1.00E+06	702.50	210.000	1.000	0.000	0.000	4900.0
10500.0	1.00E+06	651.20	200.052	1.000	0.000	0.000	11000.0
11500.0	1.00E+06	651.20	219.800	0.819	0.139	0.042	12000.0
13800.0	1.00E+06	643.70	220.800	0.606	0.302	0.092	14300.0
15000.0	1.00E+06	646.90	200.900	0.548	0.347	0.105	15500.0
16500.0	1.00E+06	639.90	165.200	0.484	0.396	0.120	17000.0
17900.0	1.00E+06	637.60	123.500	0.405	0.456	0.139	18400.0
19500.0	1.00E+06	632.00	100.200	0.399	0.461	0.140	20000.0
20600.0	1.00E+06	630.00	84.060	0.358	0.492	0.150	21100.0
22900.0	1.00E+06	625.70	61.600	0.336	0.509	0.155	23400.0
23200.0	1.00E+06	625.00	59.500	0.341	0.505	0.154	23700.0
29500.0	1.00E+06	613.00	41.900	0.284	0.549	0.167	30000.0
31600.0	1.00E+06	610.00	40.100	0.287	0.547	0.166	32100.0
49500.0	1.00E+06	587.00	36.060	0.224	0.595	0.181	50000.0
60300.0	1.00E+06	576.00	35.360	0.219	0.599	0.182	60800.0
70100.0	1.00E+06	565.00	42.660	0.175	0.633	0.192	70600.0
80100.0	1.00E+06	554.00	39.250	0.182	0.627	0.191	80600.0
114500.0	1.00E+06	515.90	37.920	0.161	0.644	0.195	115000.0

### 7.3 Input File

Torus Detonation 3 blocks, 2 ducts + 3 return bends, 180 deg - h2 generation  
 duct 3,4: vol = 22 m3, L = 48 m.  
 duct 5: bleed line, D = 0.25 m

GASFLOW

-----  
 \$innnet

```

cpnt(1:3,01) = 983.433, -57.281, -430.0, ; node #1 blk1 (PV)
cpnt(1:3,02) = -983.433, 57.281, -430.0, ; node #2 blk1 (PV)
cpnt(1:3,03) = 458.815, 122.939, -600.0, ; node #3 blk2 (DT)
cpnt(1:3,04) = -458.815, -122.939, -600.0, ; node #4 blk2 (DT)

cpnt(1:3,05) = 998.308, -58.145, 64.5, ; node #5 blk1 (PV)
cpnt(1:3,06) = 957.989, 286.803, 64.5, ; node #6 blk1 (PV)

cpnt(1:3,07) = 820.071, 219.737, 2123.5, ; node #7 blk3 (ST)
cpnt(1:3,08) = -820.071, -219.737, 2123.5, ; node #8 blk3 (ST)

cpnt(1:3,09) = 918.216, 396.074, 64.5, ; node #09 blk1 (PV)
cpnt(1:3,10) = -820.071, 219.737, 2123.5, ; node #10 blk3 (ST)

ductdef(1:12,01) = 0.0, 0.0, 45.0, 45.0, 0.0, 0.0, 1, 3, 10, 1.0, 0, 0,
ductdef(1:12,02) = 0.0, 0.0, 45.0, 45.0, 0.0, 0.0, 2, 4, 10, 1.0, 0, 0,
ductdef(1:12,03) = 0.0, 0.0, 80.0, 80.0, 0.0, 0.0, 5, 7, 10, 1.0, 4,
                    2400.0,
ductdef(1:12,04) = 0.0, 0.0, 80.0, 80.0, 0.0, 0.0, 6, 8, 10, 1.0, 4,
                    2400.0,
ductdef(1:12,05) = 0.0, 0.0, 25.0, 25.0, 0.0, 0.0, 9, 10, 10, 1.0, 4,
                    2400.0,

nwcx(1:8,01) = 20, 21, 53, 54, 1, 1, 1, 01, ; lower port bottom
nwcx(1:8,02) = 20, 21, 26, 27, 1, 1, 1, 02, ; lower port bottom
nwcx(1:8,03) = 5, 6, 1, 2, 11, 11, 2, 03, ; DT top
nwcx(1:8,04) = 5, 6, 7, 8, 11, 11, 2, 04, ; DT top

nwcx(1:8,05) = 21, 21, 53, 54, 12, 13, 1, 05, ; central port +x
nwcx(1:8,06) = 21, 21, 2, 3, 12, 13, 1, 06, ; central port +x

nwcx(1:8,07) = 9, 9, 1, 2, 10, 11, 3, 07, ; ST top
nwcx(1:8,08) = 9, 9, 7, 8, 10, 11, 3, 08, ; ST top

nwcx(1:8,10) = 9, 9, 6, 7, 10, 11, 3, 10, ; ST top
    
```

```

nwcx(1:8,09) = 21, 21, 3, 4, 12, 13, 1, 09, ; central port +x

flossdef(1:6,1) = 1, 11, 1, 0, 5.0, 5.0, ; Duct 1 flow losses
flossdef(1:6,2) = 1, 11, 2, 0, 5.0, 5.0, ; Duct 2 flow losses
flossdef(1:6,3) = 1, 11, 3, 0, 10000000.0, 10000000.0, ; Duct 3
; flow losses
flossdef(1:6,4) = 1, 11, 4, 0, 10000000.0, 10000000.0, ; Duct 4
; flow losses
flossdef(1:6,5) = 1, 11, 5, 0, 5.0, 5.0, ; Duct 5 flow losses

dampdef(1:8,1) = 1, 2, 1, 0, -0.8e+6, 0.5, 10000.0, 0.0,
dampdef(1:8,2) = 1, 2, 2, 0, -0.8e+6, 0.5, 10000.0, 0.0,
dampdef(1:8,3) = 1, 2, 3, 0, -1.5e+6, 0.5, 10000.0, 0.0,
dampdef(1:8,4) = 1, 2, 4, 0, -1.5e+6, 0.5, 10000.0, 0.0,
dampdef(1:8,5) = 1, 2, 5, 0, -0.8e+6, 0.5, 10000.0, 0.0,

netopt = 2,
kopt1d3d = 1,
iwshear = 1,
$end
$xput
  intinp(1) = 1, ; initialize by calling setupITER
  intinp(2) = 1, ; call h2ITER to generate h2 & destroy h2o
  intinp(3) = 3, ; block number for destroying h2o (SP)
  intinp(11) = 2, ; ibeg
  intinp(12) = 15, ; iend
  intinp(13) = 5, ; jbeg
  intinp(14) = 23, ; jend
  intinp(15) = 2, ; kbeg
  intinp(16) = 21, ; kend
  intinp(17) = 1, ; block number
  intinp(18) = 4, ; i cutoff

realinp(1) = 1273.000005, ; temperature cutoff
realinp(2) = 303.0, ; gas temperature for SP

nobsgeo = 1500,

geomodel(1:24,1) =+1.0, 1.0, 2.0, 0.0, 0.0, 000.0,
1.0, 1.0, 1.0, -21684, 0.0, 0.0, 0.0, 0.0, 0.0, 0.0, -404.0,
-1.0e+50, +1.0e+50, -1.0e+50, +1.0e+50, -1.0e+50, +1.0e+50, 0.0,
geomodel(1:24,2) =-1.0, 1.0, 2.0, 0.0, 0.0, 000.0,
1.0, 1.0, 1.0, -21684, 0.0, 0.0, 0.0, 0.0, 0.0, -404.0,
-1.0e+50, +1.0e+50, -1.0e+50, +1.0e+50, -1.0e+50, +1.0e+50, 2.0,
geomodel(1:24,3) =+1.0, 1.0, 2.0, 0.0, 0.0, 000.0,
1.0, 1.0, 1.0, -21684, 0.0, 0.0, 0.0, 0.0, 0.0, -404.0,
-1.0e+50, +1.0e+50, -1.0e+50, +1.0e+50, -1.0e+50, +1.0e+50, 3.0,

ignitaut = 0,
  iburn = 1,
  ifvl = 0,

  ieopt =-2,
  trange = 'low ',
  icopt = 0,
  itopt = 1,

  tmodel = 'none',
  idiffmom = 0,
  idiffme = 0,

  nrsdump = 0,
  autot = 1.0,
  cyl = 1.0,
  delt0 = 0.5e-02,
  deltmin = 0.100e-08,
  deltmax = 0.05,820.0,
0.010,824.8,
0.001,826.0,

```

```

        0.025,90000.0,
epsi0   = 1.000e-08,
epsimax = 1.000e-08,
epsimin = 1.000e-08,
iobpl   = 1,
itdowndt = 500,
itupdt  = 500,
itmax   = 1000,
lpr     = 1,
maxcyc  = 2050000000,
ittyfreq = 100,
pltdt   = 5.0e+2,
prtdt   = 91000.,
twfin   = 21000.0,
tddt    = 824.0,825.0,
        076.0, 0901.0,
        100.0, 1001.0,
        1500.0, 99999.0,
velmx   = 5.0,
ibe     = 1,
ibw     = 1,
ibn     = 4,
ibs     = 4,
ibt     = 1,
ibb     = 1,

gz      = -980.0,

mat     = 'h2', 'h2o', 'n2', 'o2',

gasdef(1:40,1)= 1,'im1', 1,'jm1', 1,'km1', 1,115000.0 , 503.00, 2,
                0., 0., 'n2', 1.000, 'o2', 0.000, 'h2', 0.000, 22*0.0,
                ;blk 1 (VV)
gasdef(1:40,2)= 1,'im1', 1,'jm1', 1,'km1', 1, 5000.0 ,1273.00001, 2,
                0., 0., 'n2', 1.000, 'o2', 0.000, 'h2', 0.000, 22*0.0,
                ;blk 1 (VV)
gasdef(1:40,3)= 1,'im1', 1,'jm1', 1,'km1', 1, 5000.0 ,1273.00, 2,
                0., 0., 'n2', 1.000, 'o2', 0.000, 'h2', 0.000, 22*0.0,
                ;blk 1 (VV)
gasdef(1:40,4)= 1,'im1', 1, 4, 1,'km1', 1, 5000.0 , 503.00, 2,
                0., 0., 'n2', 1.000, 'o2', 0.000, 'h2', 0.000, 22*0.0,
                ;blk 1 (VV)
gasdef(1:40,5)= 1,'im1', 23, 55, 1,'km1', 1, 5000.0 , 503.00, 2,
                0., 0., 'n2', 1.000, 'o2', 0.000, 'h2', 0.000, 22*0.0,
                ;blk 1 (VV)
gasdef(1:40,6)= 1,'im1', 1,'jm1', 1,'km1', 2, 4.200e+04, 303.00, 2,
                0., 0., 'n2', 1.000, 'o2', 0.000, 'h2', 0.000, 22*0.0,
                ;blk 2 (DT)
gasdef(1:40,7)= 1,'im1', 1,'jm1', 1,'km1', 3, 4.200e+04, 303.00, 2,
                0., 0., 'n2', 1.000, 'o2', 0.000, 'h2', 0.000, 22*0.0,
                ;blk 3 (ST)

gasdef(1:40,8)= 2, 12, 1, 0, 0, 0, 0, 4.200e+04, 303.00, 2,
                0., 0., 'n2', 1.000, 'o2', 0.000, 'h2', 0.000, 22*0.0,
                ; duct 1

gasdef(1:40,9)= 2, 12, 2, 0, 0, 0, 0, 4.200e+04, 303.00, 2,
                0., 0., 'n2', 1.000, 'o2', 0.000, 'h2', 0.000, 22*0.0,
                ; duct 2

gasdef(1:40,10)= 2, 12, 3, 0, 0, 0, 0, 4.200e+04, 303.00, 2,
                0., 0., 'n2', 1.000, 'o2', 0.000, 'h2', 0.000, 22*0.0,
                ; duct 3

gasdef(1:40,11)= 2, 12, 4, 0, 0, 0, 0, 4.200e+04, 303.00, 2,
                0., 0., 'n2', 1.000, 'o2', 0.000, 'h2', 0.000, 22*0.0,
                ; duct 4

gasdef(1:40,12)= 2, 12, 5, 0, 0, 0, 0, 4.200e+04, 303.00, 2,

```

```

0., 0., 'n2', 1.000, 'o2', 0.000, 'h2', 0.000, 22*0.0,
; duct 5

gasdef(1:40,13)= 0, 2, 1, 0, 0, 0, 0, 5000.0, 503.00, 2,
0., 0., 'n2', 1.000, 'o2', 0.000, 'h2', 0.000, 22*0.0,
; duct 1

gasdef(1:40,14)= 0, 2, 2, 0, 0, 0, 0, 5000.0, 503.00, 2,
0., 0., 'n2', 1.000, 'o2', 0.000, 'h2', 0.000, 22*0.0,
; duct 2

gasdef(1:40,15)= 0, 2, 3, 0, 0, 0, 0, 5000.0, 503.00, 2,
0., 0., 'n2', 1.000, 'o2', 0.000, 'h2', 0.000, 22*0.0,
; duct 3

gasdef(1:40,16)= 0, 2, 4, 0, 0, 0, 0, 5000.0, 503.00, 2,
0., 0., 'n2', 1.000, 'o2', 0.000, 'h2', 0.000, 22*0.0,
; duct 4

gasdef(1:40,17)= 0, 2, 5, 0, 0, 0, 0, 5000.0, 503.00, 2,
0., 0., 'n2', 1.000, 'o2', 0.000, 'h2', 0.000, 22*0.0,
; duct 5

holes(1:13,01)= 1, 21, 02, 04, 01, 04, 1, 0, 0, -1, -1, 0, -1,
holes(1:13,02)= 1, 21, 02, 04, 09, 13, 1, 0, 0, -1, -1, -1, -1,
holes(1:13,03)= 1, 21, 05, 07, 01, 04, 1, 0, 0, -1, -1, 0, -1,
holes(1:13,04)= 1, 21, 05, 07, 09, 13, 1, 0, 0, -1, -1, -1, -1,
holes(1:13,05)= 1, 21, 08, 10, 01, 04, 1, 0, 0, -1, -1, 0, -1,
holes(1:13,06)= 1, 21, 08, 10, 09, 13, 1, 0, 0, -1, -1, -1, -1,
holes(1:13,07)= 1, 21, 11, 13, 01, 04, 1, 0, 0, -1, -1, 0, -1,
holes(1:13,08)= 1, 21, 11, 13, 09, 13, 1, 0, 0, -1, -1, -1, -1,
holes(1:13,09)= 1, 21, 14, 16, 01, 04, 1, 0, 0, -1, -1, 0, -1,
holes(1:13,10)= 1, 21, 14, 16, 09, 13, 1, 0, 0, -1, -1, -1, -1,
holes(1:13,11)= 1, 21, 17, 19, 01, 04, 1, 0, 0, -1, -1, 0, -1,
holes(1:13,12)= 1, 21, 17, 19, 09, 13, 1, 0, 0, -1, -1, -1, -1,
holes(1:13,13)= 1, 21, 20, 22, 01, 04, 1, 0, 0, -1, -1, 0, -1,
holes(1:13,14)= 1, 21, 20, 22, 09, 13, 1, 0, 0, -1, -1, -1, -1,
holes(1:13,15)= 1, 21, 23, 25, 01, 04, 1, 0, 0, -1, -1, 0, -1,
holes(1:13,16)= 1, 21, 23, 25, 09, 13, 1, 0, 0, -1, -1, -1, -1,
holes(1:13,17)= 1, 21, 26, 28, 01, 04, 1, 0, 0, -1, -1, 0, -1,
holes(1:13,18)= 1, 21, 26, 28, 09, 13, 1, 0, 0, -1, -1, -1, -1,
holes(1:13,19)= 1, 21, 29, 31, 01, 04, 1, 0, 0, -1, -1, 0, -1,
holes(1:13,20)= 1, 21, 29, 31, 09, 13, 1, 0, 0, -1, -1, -1, -1,
holes(1:13,21)= 1, 21, 32, 34, 01, 04, 1, 0, 0, -1, -1, 0, -1,
holes(1:13,22)= 1, 21, 32, 34, 09, 13, 1, 0, 0, -1, -1, -1, -1,
holes(1:13,23)= 1, 21, 35, 37, 01, 04, 1, 0, 0, -1, -1, 0, -1,
holes(1:13,24)= 1, 21, 35, 37, 09, 13, 1, 0, 0, -1, -1, -1, -1,
holes(1:13,25)= 1, 21, 38, 40, 01, 04, 1, 0, 0, -1, -1, 0, -1,
holes(1:13,26)= 1, 21, 38, 40, 09, 13, 1, 0, 0, -1, -1, -1, -1,
holes(1:13,27)= 1, 21, 41, 43, 01, 04, 1, 0, 0, -1, -1, 0, -1,
holes(1:13,28)= 1, 21, 41, 43, 09, 13, 1, 0, 0, -1, -1, -1, -1,
holes(1:13,29)= 1, 21, 44, 46, 01, 04, 1, 0, 0, -1, -1, 0, -1,
holes(1:13,30)= 1, 21, 44, 46, 09, 13, 1, 0, 0, -1, -1, -1, -1,
holes(1:13,31)= 1, 21, 47, 49, 01, 04, 1, 0, 0, -1, -1, 0, -1,
holes(1:13,32)= 1, 21, 47, 49, 09, 13, 1, 0, 0, -1, -1, -1, -1,
holes(1:13,33)= 1, 21, 50, 52, 01, 04, 1, 0, 0, -1, -1, 0, -1,
holes(1:13,34)= 1, 21, 50, 52, 09, 13, 1, 0, 0, -1, -1, -1, -1,
holes(1:13,35)= 1, 21, 53, 55, 01, 04, 1, 0, 0, -1, -1, 0, -1,
holes(1:13,36)= 1, 21, 53, 55, 09, 13, 1, 0, 0, -1, -1, -1, -1,

mobs(1:8,1)= 1, 3, 1, 'jm1', 20, 21, 1, 0,
mobs(1:8,2)= 1, 2, 1, 'jm1', 19, 20, 1, 0,

; the following input is required for the superheated steam source and to
; isentropically expand it to the torus low pressure

tshift_sortam = 10.0,
sortami = 2,
holes(1:13,37) = 15, 16, 13, 14, 10, 11, 1, 1, 0, 0, 0, 0, 0, 0,

```

```

; reservoir
gasdef(1:18,18) = 15, 16, 13, 14, 10, 11, 1, -1,-2, -401, 0.,
30000000.,
'h2o', -304, ; reservoir
'n2' , -305, ; reservoir
'o2' , -306 ; reservoir
subsodef(1:7,1) = 15, 16, 13, 14, 10, 11, 1,
zeroddef(1:7,1) = 15, 15, 13, 14, 10, 11, 1,
vbc(1:10,1) = 15, 15, 13, 14, 10, 11, 1, -1, 0.0, 300000000.0,
vvalue = 0.0, 30000.0, 30000.0,
pref = -17131101, ; i j k iblk pressure reference location
gamma = 1.28,

; look at using vbc to develop a critical flow model
; vbc(1:10,2) = 2, 2, 1, 0,0,0, 0, 102, 0.0, 99999.9,
; vbc(1:10,3) = 2, 2, 2, 0,0,0, 0, 103, 0.0, 99999.9,
$end

-----
h e a t - t r a n s f e r
-----
$rheat
ihtflag = 0,
$end

-----
m e s h
-----
$meshgn
iblock = 1,
nkx = 1,
xl(1) = 404.0, xc(1) = 404.0, nxl(1) = 0, nxr(1) = 20, dxmn(1) = 9999.,
xl(2) = 1000.0,
nky = 1,
yl(1) = 6.667, yc(1) = 6.67, nyl(1) = 0, nyr(1) = 54, dymn(1) = 9999.,
yl(2) = 366.667,
nkz = 1,
zl(1) = -430.0, zc(1) = -430.0, nzl(1) = 0, nZR(1) = 20, dzmn(1) = 9999.,
zl(2) = 430.0,
$end

$meshgn
iblock = 2,
nkx = 1,
xl(1) = 0.0, xc(1) = 0.0, nxl(1) = 0, nxr(1) = 05, dxmn(1) = 9999.,
xl(2) = 500.0,
nky = 1,
yl(1) = 0.0, yc(1) = 0.0, nyl(1) = 0, nyr(1) = 12, dymn(1) = 9999.,
yl(2) = 360.0,
nkz = 1,
zl(1) = -1100.0, zc(1) = -1100.0, nzl(1) = 0, nZR(1) = 10, dzmn(1) = 9999.,
zl(2) = -600.0,
$end

$meshgn
iblock = 3,
nkx = 1,
xl(1) = 0.0, xc(1) = 0.0, nxl(1) = 0, nxr(1) = 08, dxmn(1) = 9999.,
xl(2) = 849.0,
nky = 1,
yl(1) = 0.0, yc(1) = 0.0, nyl(1) = 0, nyr(1) = 12, dymn(1) = 9999.,
yl(2) = 360.0,
nkz = 1,
zl(1) = 1620.0, zc(1) = 1620.0, nzl(1) = 0, nZR(1) = 10, dzmn(1) = 9999.,
zl(2) = 2150.0,
$end

-----
g r a p h i c s

```

```

-----
$grafic
  thdt = 5.0,

  thp(1:6,1) = 15, 14, 11, 1, 'un', 0,
  thp(1:6,2) = 15, 14, 11, 1, 'mdotx', 0,
  thp(1:6,3) = 16, 14, 11, 1, 'pn', 0,
  thp(1:6,4) = 16, 14, 11, 1, 'tk', 0,
  thp(1:6,5) = 02, 01, 00, 00, 'un', 0,
  thp(1:6,6) = 02, 02, 00, 00, 'un', 0,
  thp(1:6,7) = 02, 03, 00, 00, 'un', 0,
  thp(1:6,8) = 02, 05, 00, 00, 'un', 0,
  thp(1:6,9) = 02, 01, 00, 00, 'delpx', 0,
  thp(1:6,10) = 02, 02, 00, 00, 'delpx', 0,
  thp(1:6,11) = 02, 03, 00, 00, 'delpx', 0,
  thp(1:6,12) = 02, 05, 00, 00, 'delpx', 0,
  thp(1:6,13) = 02, 02, 02, 01, 'pn', 0,
  thp(1:6,14) = 02, 02, 02, 02, 'pn', 0,
  thp(1:6,15) = 02, 02, 02, 03, 'pn', 0,
  thp(1:6,16) = 02, 02, 02, 03, 'delt', 0,
  thp(1:6,17) = 11, 01, 00, 00, 'un', 0,
  thp(1:6,18) = 11, 02, 00, 00, 'un', 0,
  thp(1:6,19) = 11, 03, 00, 00, 'un', 0,
  thp(1:6,20) = 11, 05, 00, 00, 'un', 0,

  pnt(1:4,1) = 1, 14, 1, 1, ; rz top
  pnt(1:4,2) = 'im1', 14, 'km1', 1,
  pnt(1:4,3) = 1, 15, 1, 1, ; rz left, no port
  pnt(1:4,4) = 'im1', 15, 'km1', 1,
  pnt(1:4,5) = 1, 41, 1, 1, ; rz bottom
  pnt(1:4,6) = 'im1', 41, 'km1', 1,
  pnt(1:4,7) = 1, 1, 2, 1, ; xy bot
  pnt(1:4,8) = 'im1','jml', 2, 1,
  pnt(1:4,9) = 1, 1, 11, 1, ; xy med
  pnt(1:4,10) = 'im1','jml', 11, 1,
  pnt(1:4,11) = 1, 1, 20, 1, ; xy top
  pnt(1:4,12) = 'im1','jml', 20, 1,
  pnt(1:4,13) = 1, 27, 1, 1, ; rz left, port
  pnt(1:4,14) = 'im1', 27, 'km1', 1,

  pnt(1:4,15) = 1, 1, 0, 0, ; duct 1
  pnt(1:4,16) = 11, 1, 0, 0, ; duct 1
  pnt(1:4,17) = 1, 2, 0, 0, ; duct 2
  pnt(1:4,18) = 11, 2, 0, 0, ; duct 2
  pnt(1:4,19) = 1, 3, 0, 0, ; duct 3
  pnt(1:4,20) = 11, 3, 0, 0, ; duct 3
  pnt(1:4,21) = 1, 4, 0, 0, ; duct 4
  pnt(1:4,22) = 11, 4, 0, 0, ; duct 4
  pnt(1:4,23) = 1, 5, 0, 0, ; duct 5
  pnt(1:4,24) = 11, 5, 0, 0, ; duct 5
  pnt(1:4,25) = 1, 8, 1, 2, ;
  pnt(1:4,26) = 6, 8, 11, 2, ;
  pnt(1:4,27) = 6, 8, 1, 2, ;
  pnt(1:4,28) = 6, 8, 11, 2, ;

  v2d(1:3,1) = 1, 2, 1,
  v2d(1:3,2) = 9, 10, 1,
  v2d(1:3,3) = 7, 08, 1,
  v2d(1:3,4) = 13, 14, 1,
  v2d(1:3,5) = 25, 26, 1,

  c2d(1:4,1) = 1, 2, 'tk', 0,
  c2d(1:4,2) = 3, 4, 'tk', 0,
  c2d(1:4,3) = 5, 6, 'tk', 0,
  c2d(1:4,4) = 7, 8, 'tk', 0,
  c2d(1:4,5) = 9, 10, 'tk', 0,
  c2d(1:4,6) = 11, 12, 'tk', 0,
  c2d(1:4,7) = 13, 14, 'tk', 0,
  c2d(1:4,8) = 7, 08, 'pn', 0,

```

```
c2d(1:4,9) = 9, 10, 'pn', 0,
c2d(1:4,10) = 13, 14, 'pn', 0,
c2d(1:4,11) = 25, 26, 'pn', 0,

p1d(1:4,1) = 15, 16, 'un', 0, ; duct 1
p1d(1:4,2) = 17, 18, 'un', 0, ; duct 2
p1d(1:4,3) = 19, 20, 'un', 0, ; duct 3
p1d(1:4,4) = 21, 22, 'un', 0, ; duct 4
p1d(1:4,5) = 23, 24, 'un', 0, ; duct 5
p1d(1:4,6) = 15, 16, 'pn', 0, ; duct 1
p1d(1:4,7) = 17, 18, 'pn', 0, ; duct 2
p1d(1:4,8) = 19, 20, 'pn', 0, ; duct 3
p1d(1:4,9) = 21, 22, 'pn', 0, ; duct 4
p1d(1:4,10) = 23, 24, 'pn', 0, ; duct 5
p1d(1:4,11) = 15, 16, 'rn', 0, ; duct 1
p1d(1:4,12) = 17, 18, 'rn', 0, ; duct 2
p1d(1:4,13) = 15, 16, 'tk', 0, ; duct 1
p1d(1:4,14) = 17, 18, 'tk', 0, ; duct 2
p1d(1:4,15) = 27, 28, 'wn', 0, ;
p1d(1:4,16) = 27, 28, 'pn', 0, ;

$end

$special

$end
$parts

$end
; ----- end of data -----
; -----
```

Figures

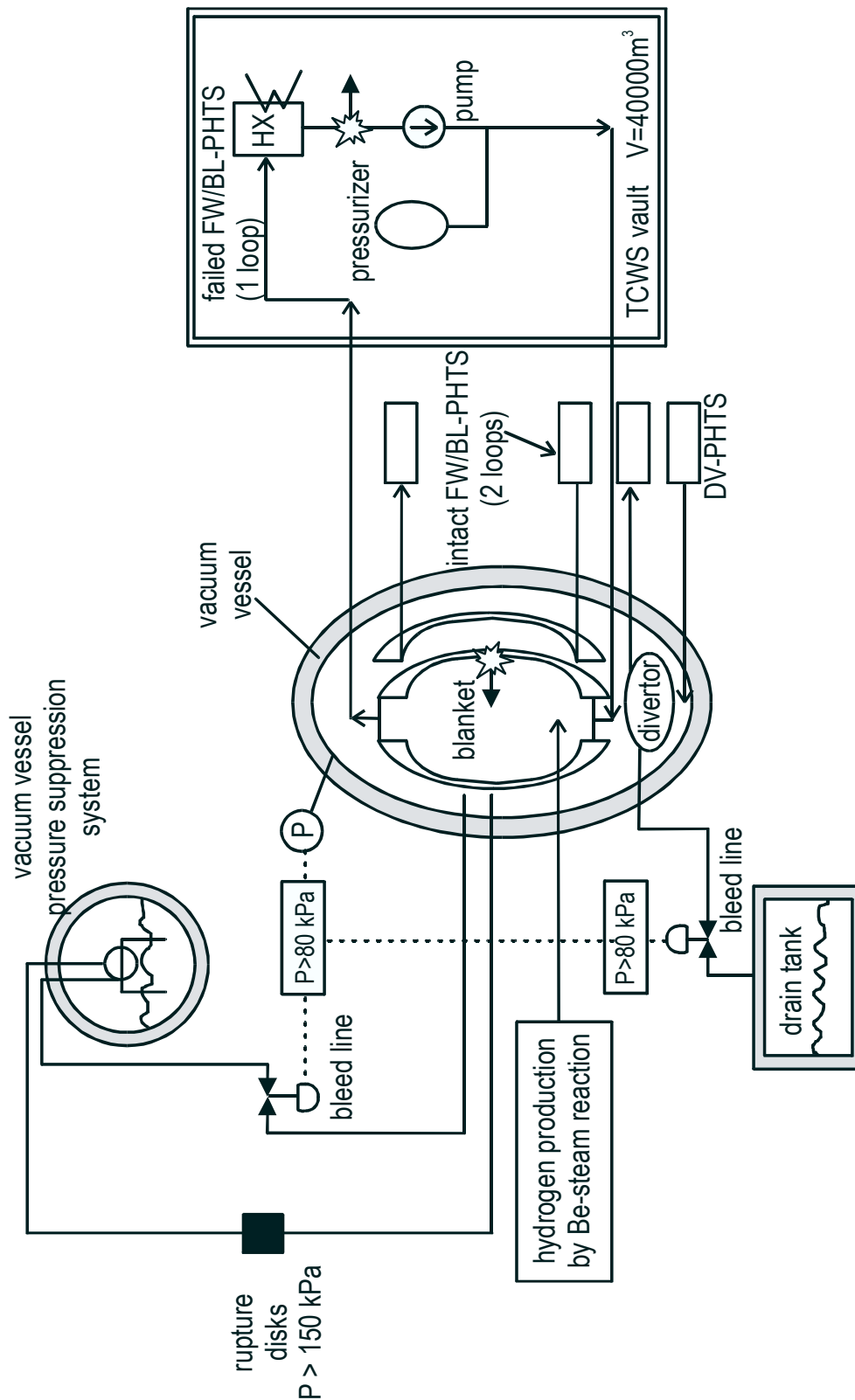


Figure 1 Ex-vessel LOCA scenario without plasma shut-down, leading to in-vessel break and injection of steam and air into the VV. Burst membranes open flow paths to the safety systems when the differential pressure exceeds 0.8 bar.

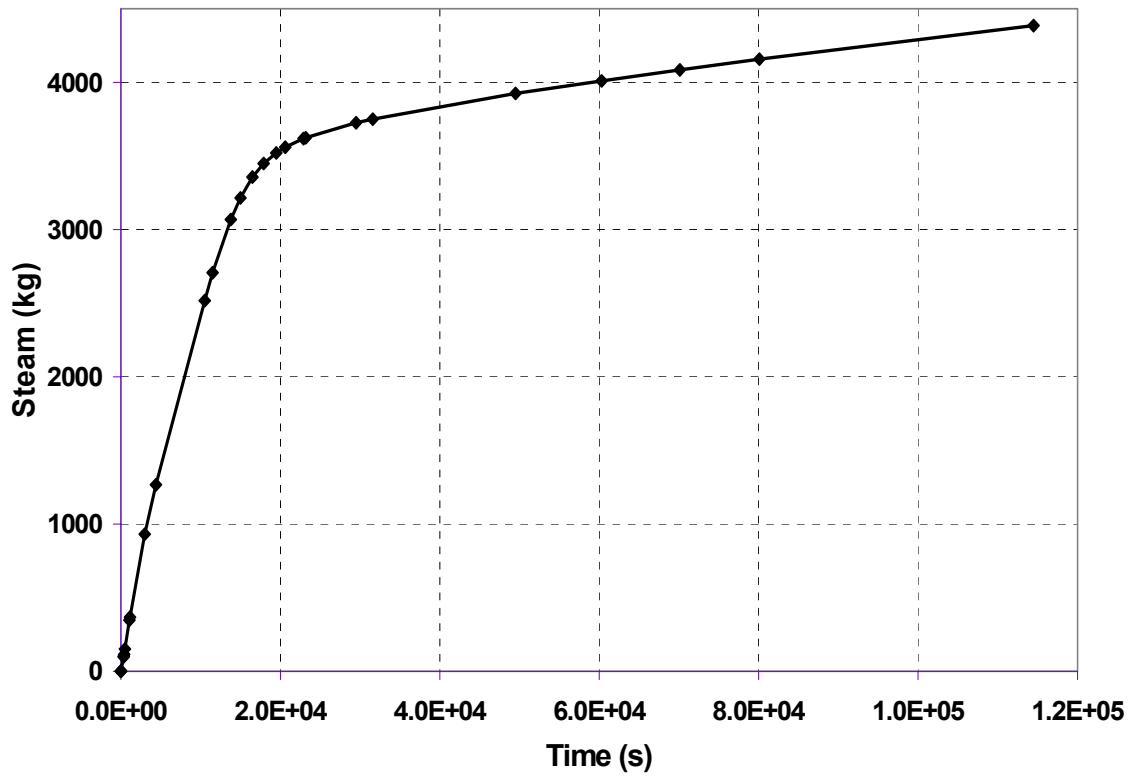


Figure 2: Accumulated steam mass released into the ITER-FEAT vacuum vessel (MELCOR result [3]).

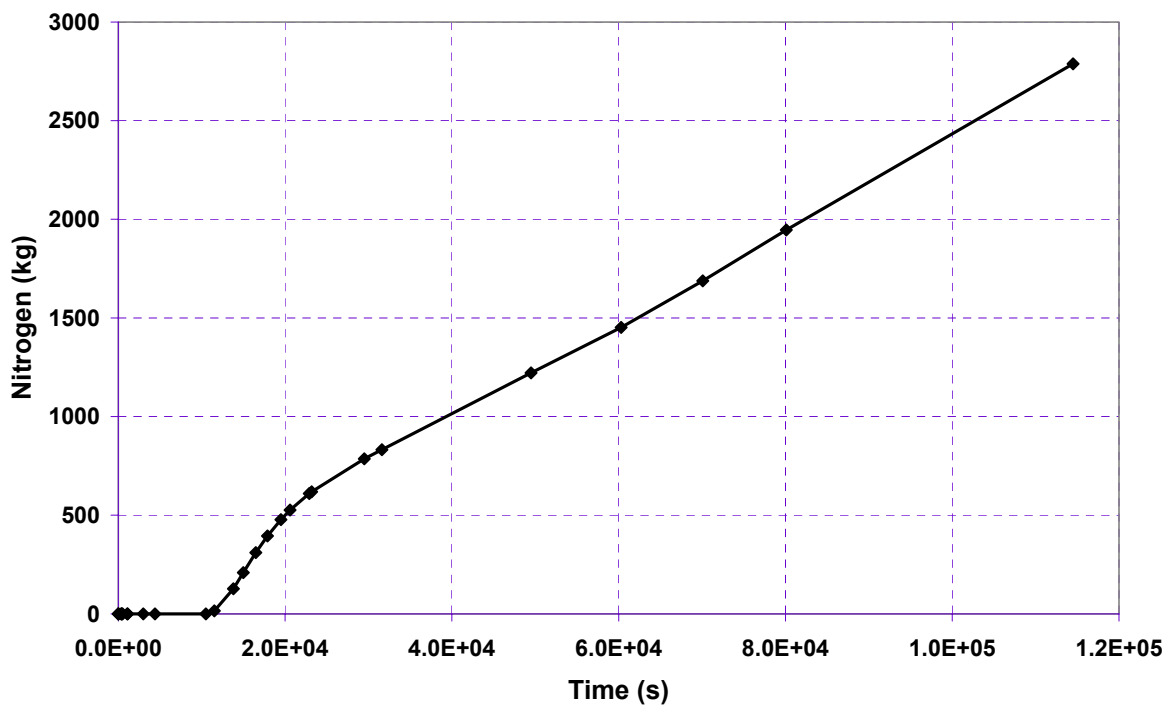


Figure 3: Accumulated nitrogen mass released into the ITER-FEAT vacuum vessel (MELCOR result [3]).

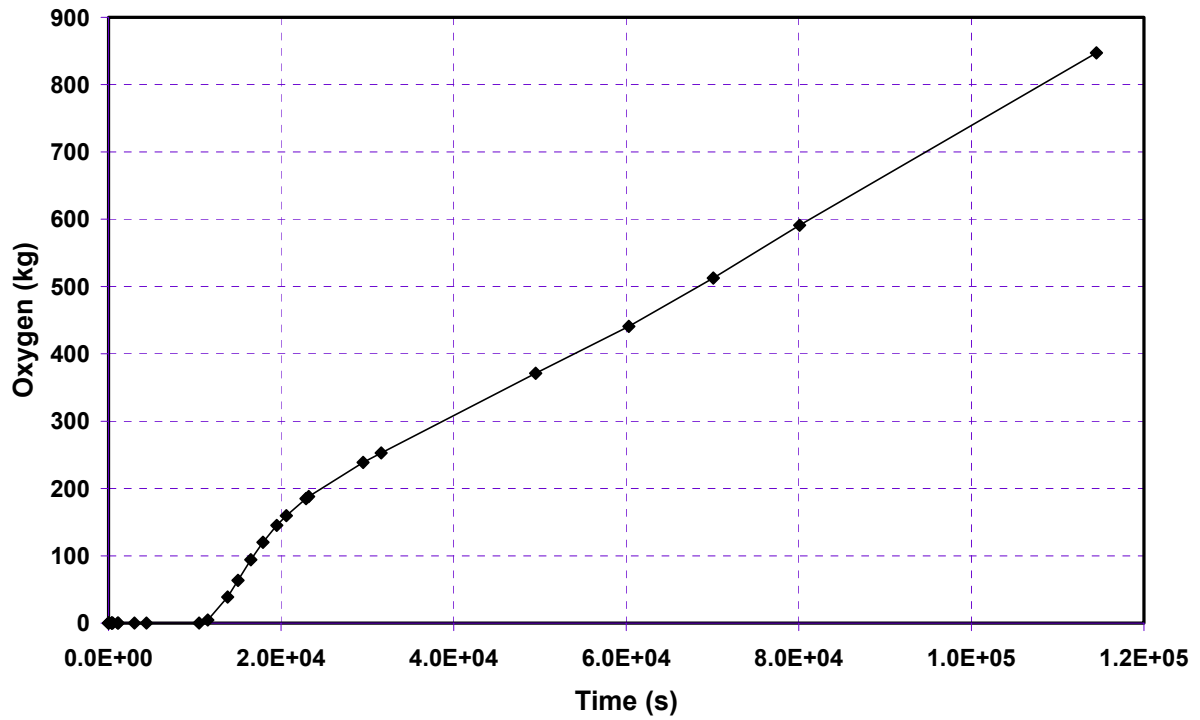


Figure 4: Accumulated oxygen mass released into the ITER-FEAT vacuum vessel (MELCOR result [3]).

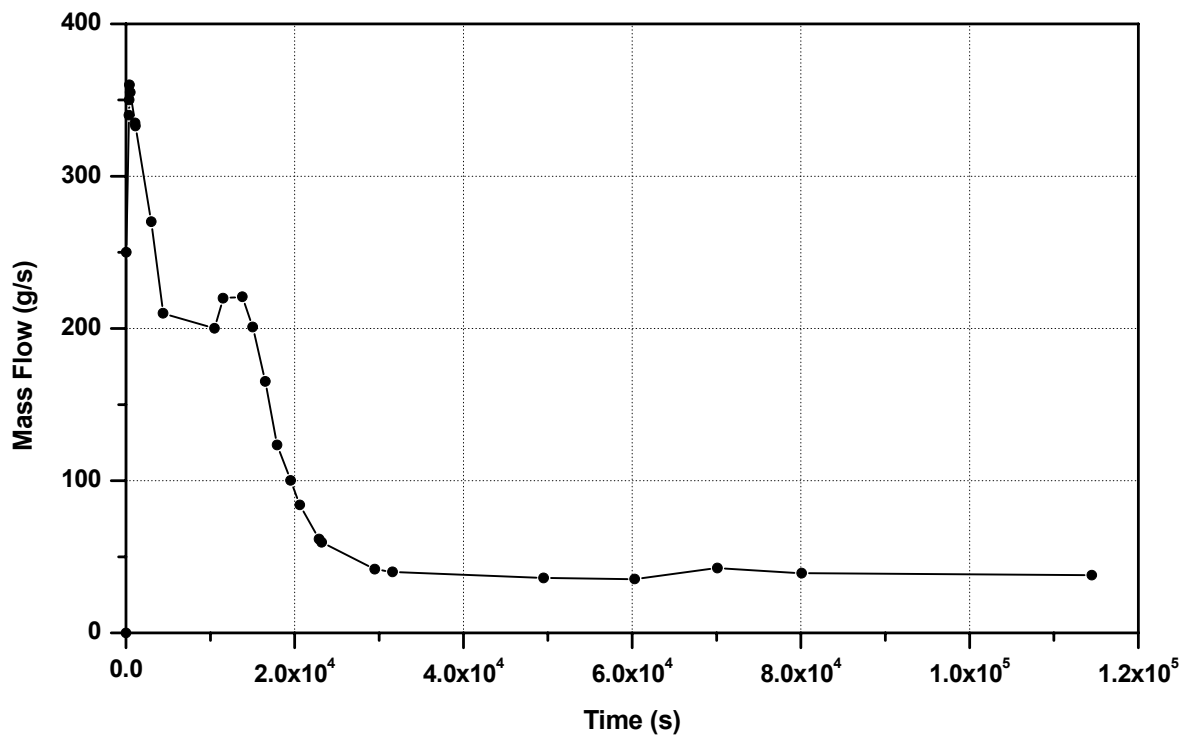


Figure 5: Total mass flow rate of steam and air entering the ITER-FEAT vacuum vessel (MELCOR result [3]).

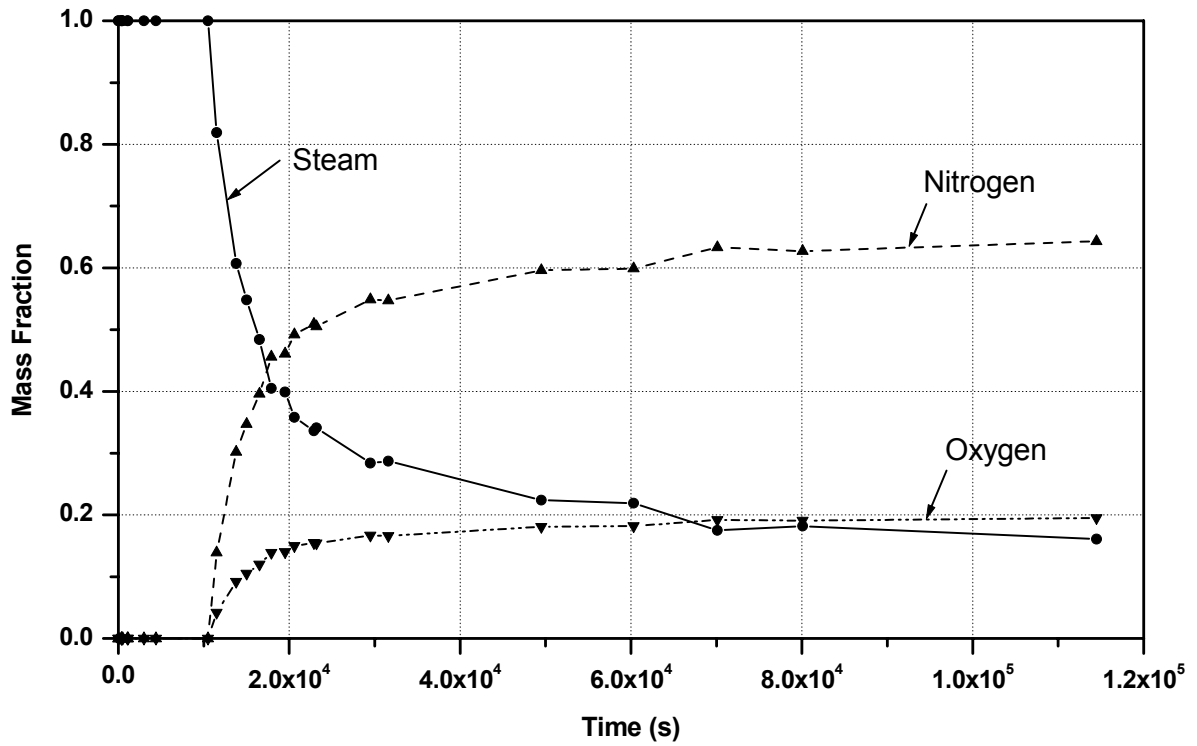


Figure 6: Mass fractions of steam, nitrogen, and oxygen flowing into the ITER-FEAT vacuum vessel (MELCOR result [3]).

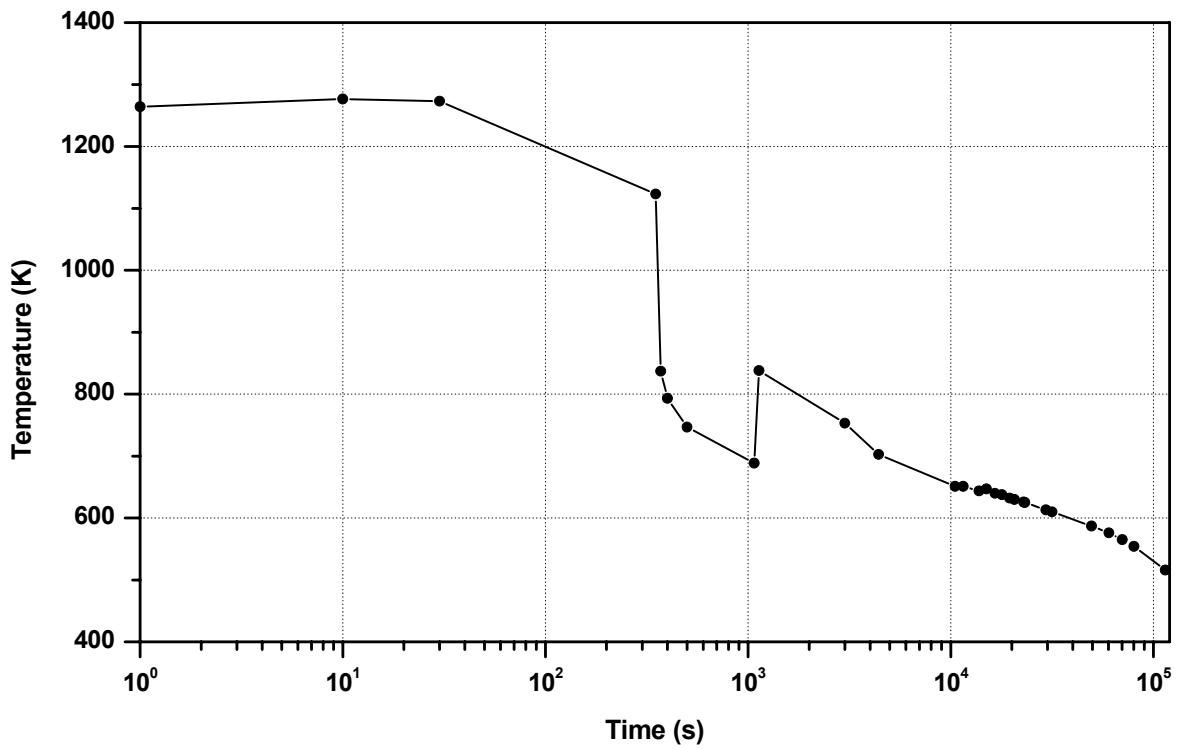


Figure 7: Temperature of steam and air flow, logarithmic time scale (MELCOR result [3]).

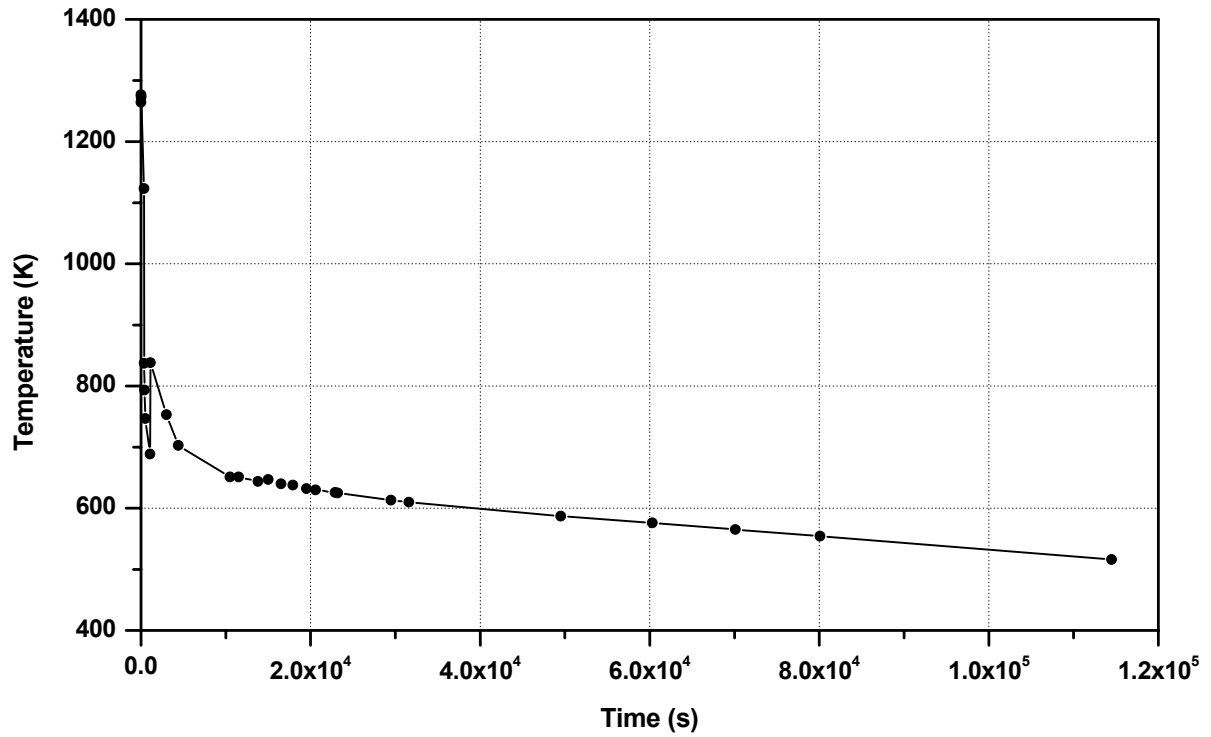


Figure 8: Temperature of steam and air flow, linear time scale (MELCOR result [3]).

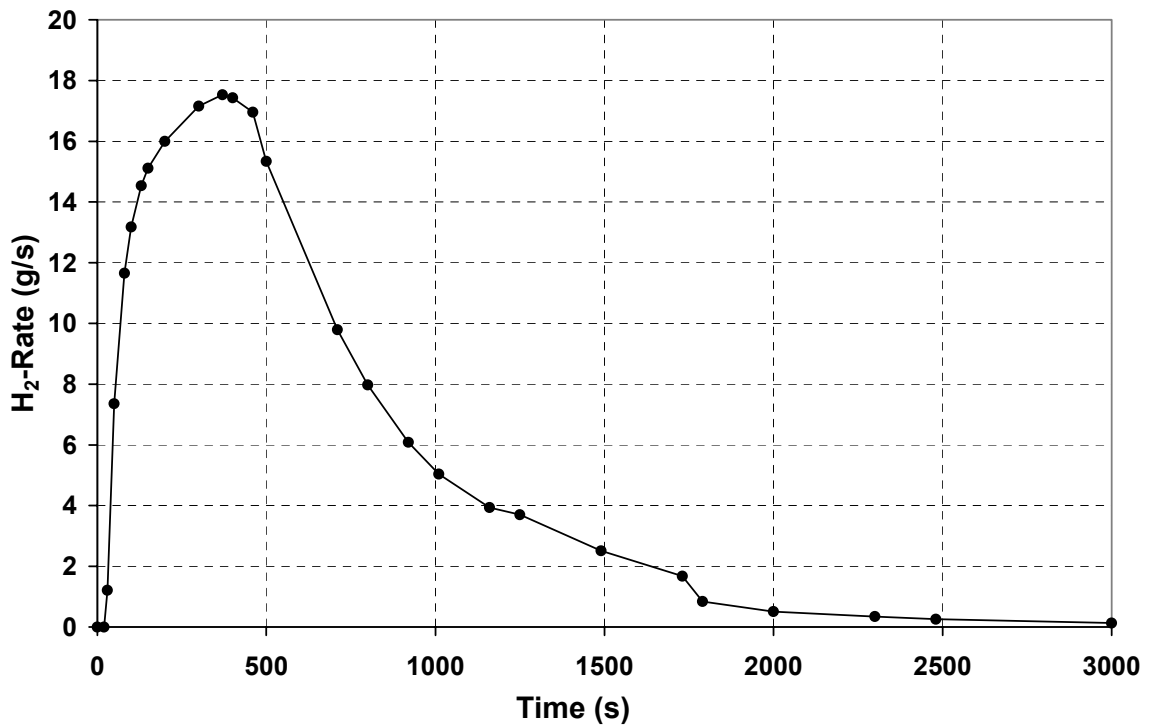


Figure 9: Hydrogen rate produced in the vacuum vessel due to Be-steam reaction (MELCOR result [3]).

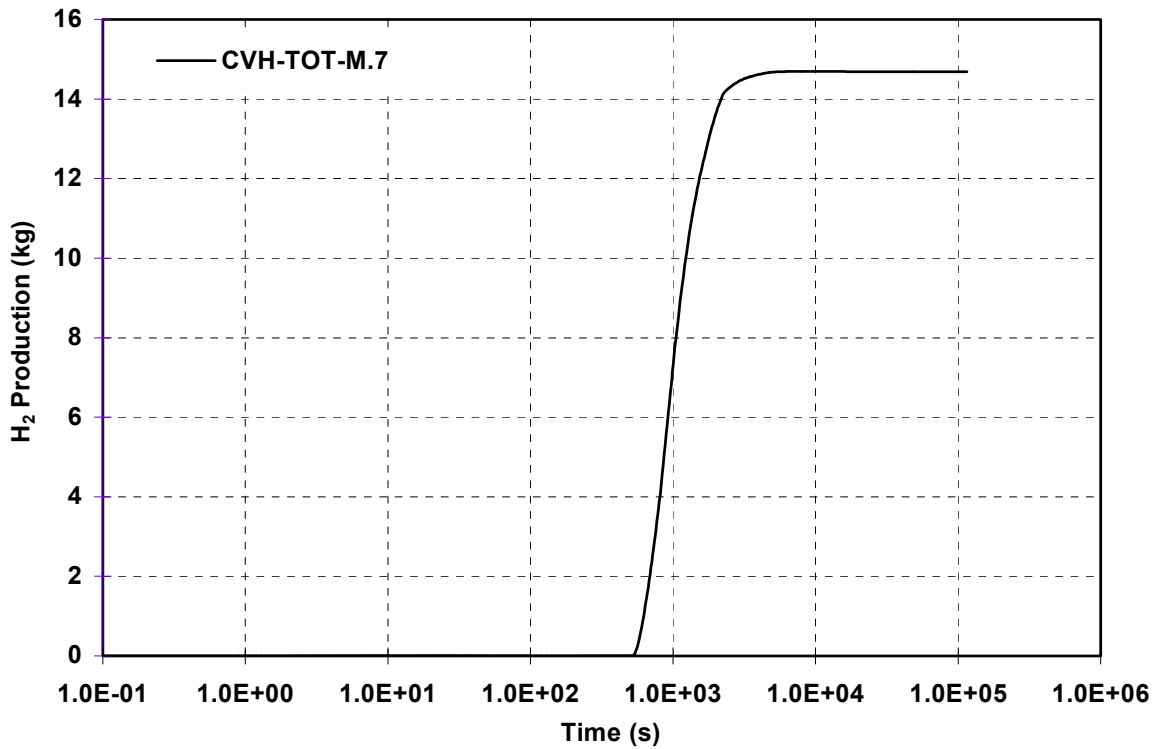


Figure 10: Accumulated hydrogen mass released into the ITER-FEAT vacuum vessel (MELCOR result [3]).

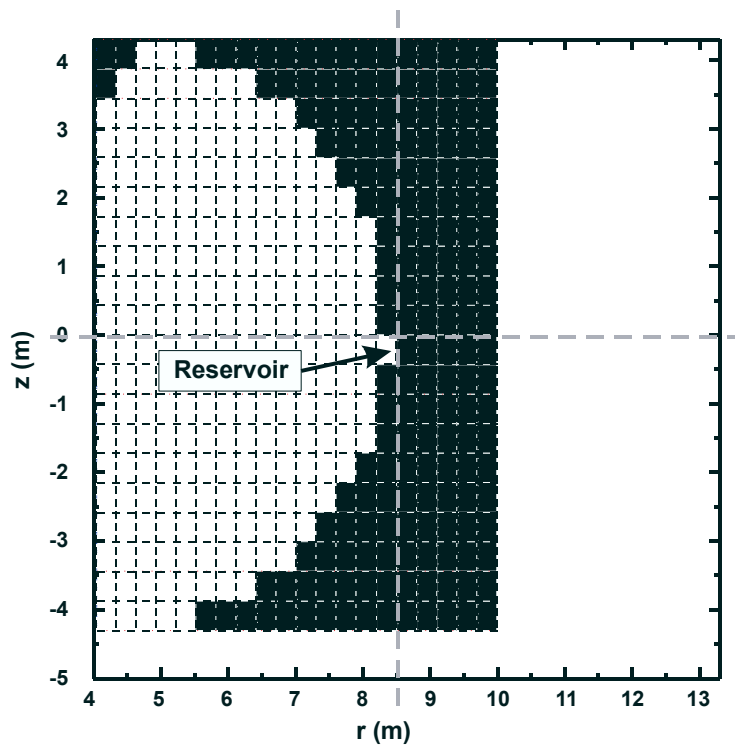


Figure 11: Vertical r-z cut through the vacuum vessel showing the location of the source reservoir.

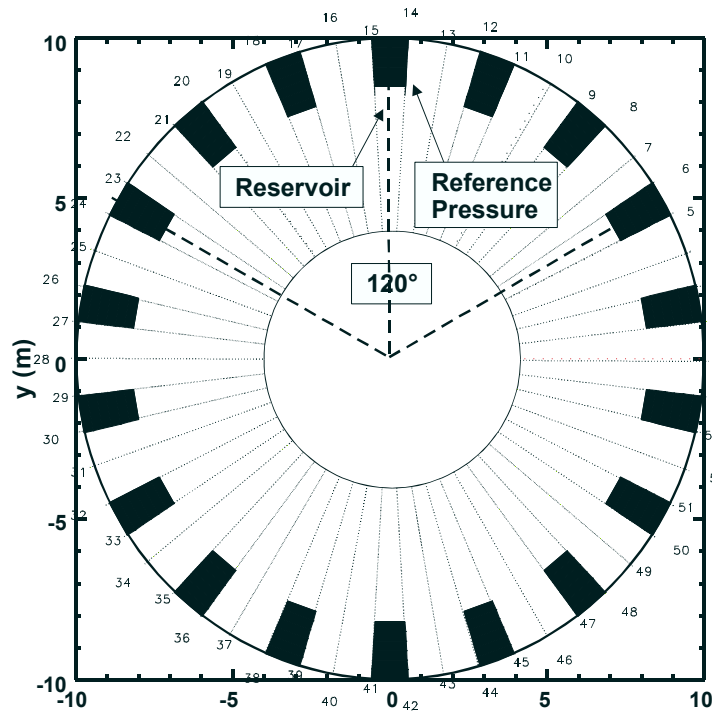


Figure 12: Horizontal r-θ cut through the vacuum vessel showing the location of the source reservoir and reference pressure position.

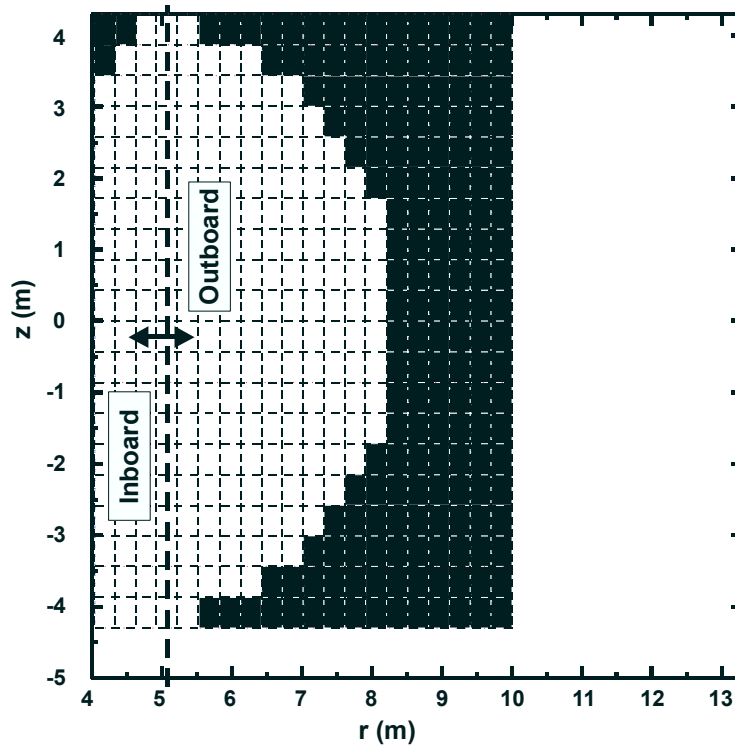


Figure 13: Vertical r-z cut through the vacuum vessel showing the locations of the inboard and outboard beryllium surfaces.

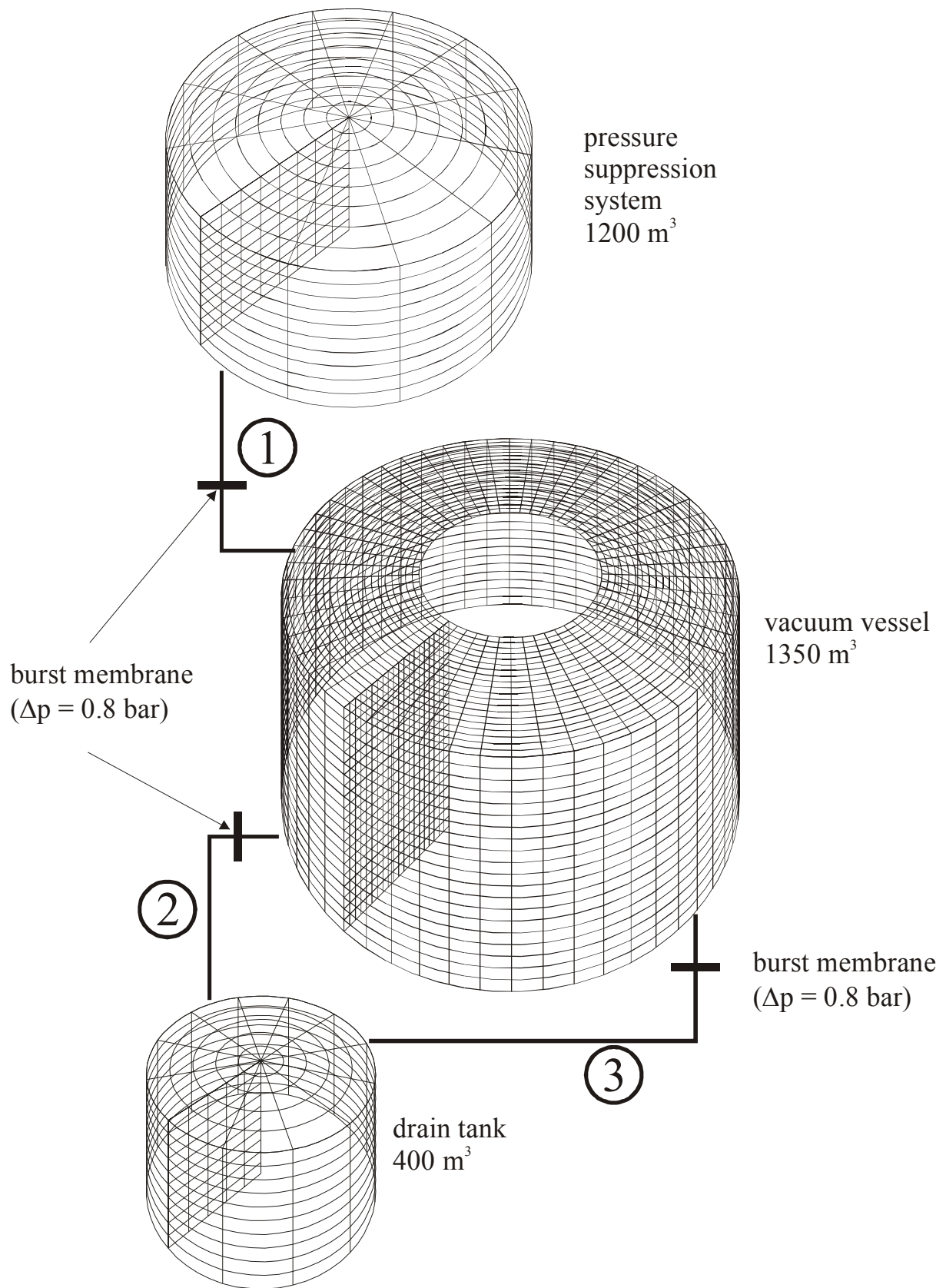


Figure 14: GASFLOW grids for the ITER-FEAT model

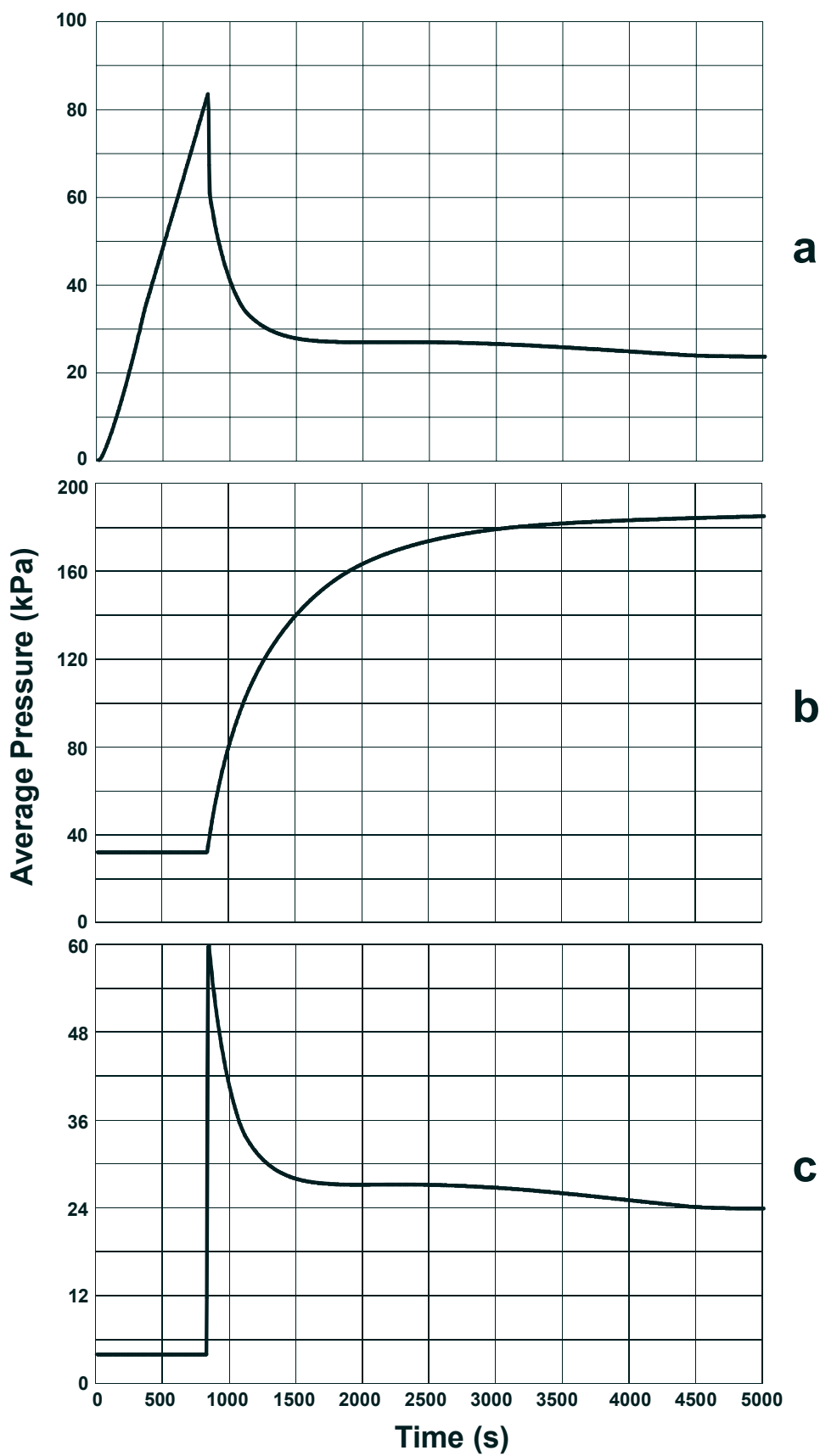


Figure 15: Calculated average pressures in the modeled ITER-FEAT vessels: a) vacuum vessel, b) suppression pool, c) drain tank. Initial phase of accident up to 5,000 seconds.

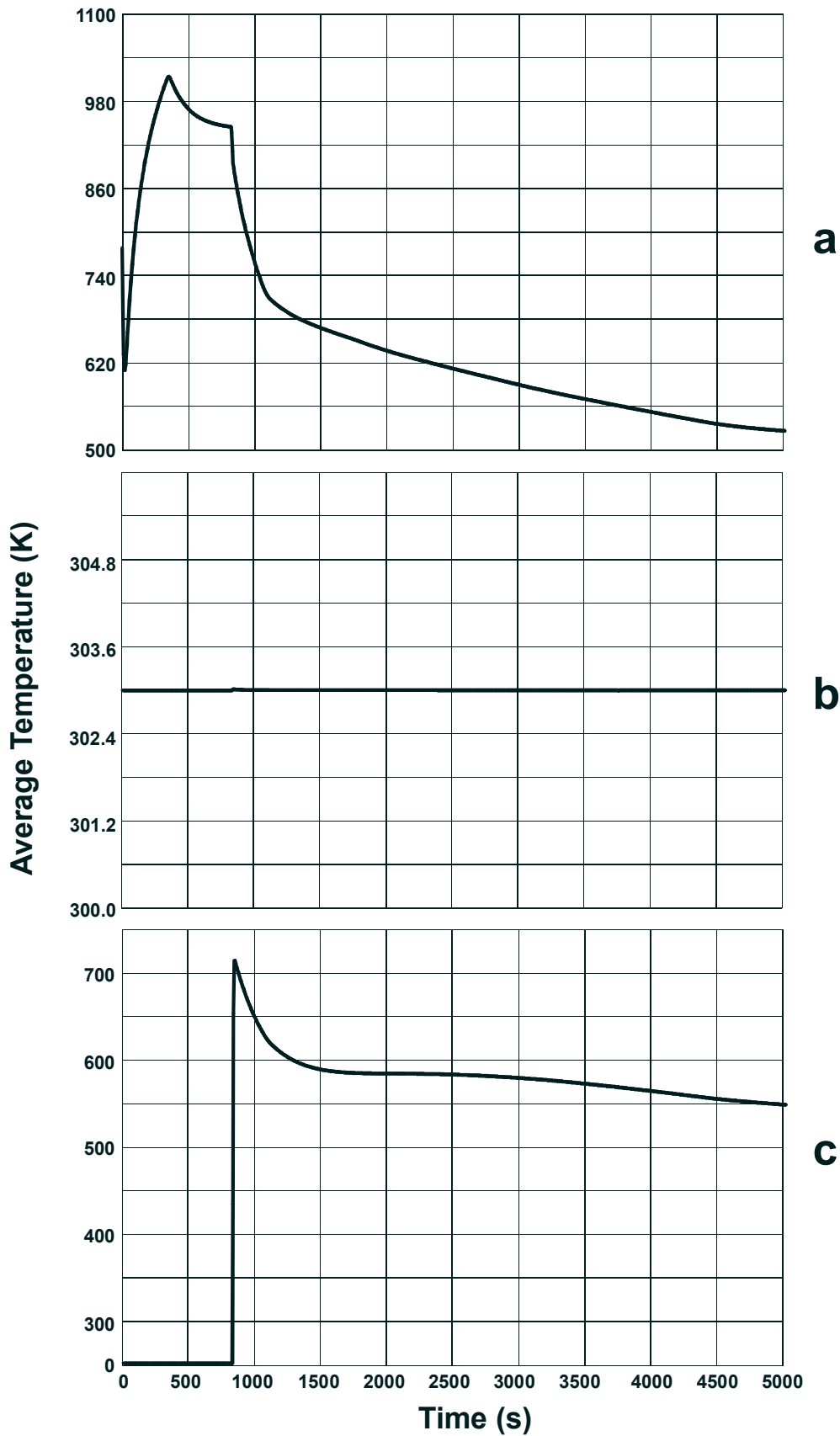


Figure 16: Calculated average temperatures in the modeled ITER-FEAT vessels:  
 a) vacuum vessel, b) suppression pool, c) drain tank.  
 Initial phase of accident up to 5,000 seconds

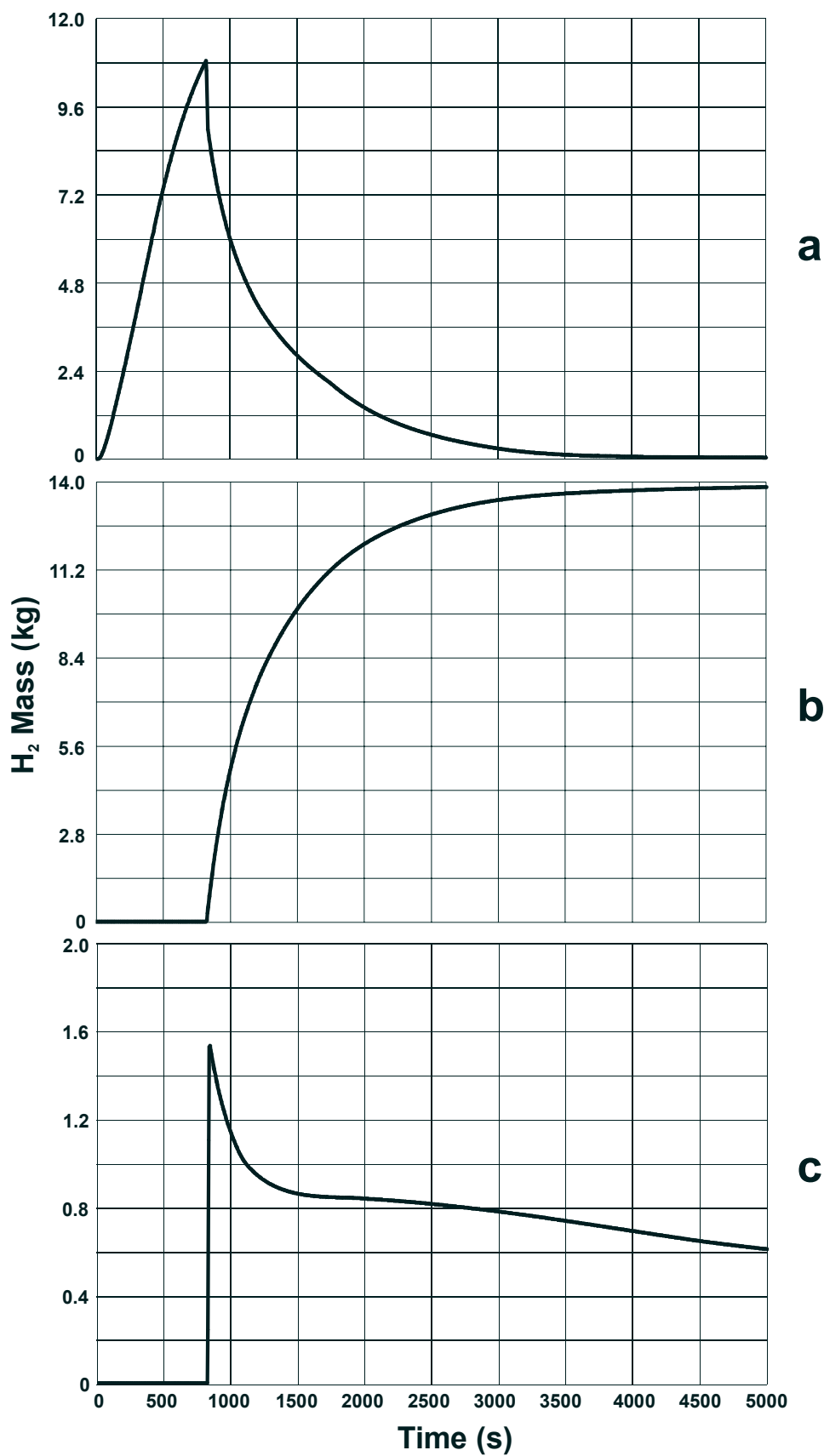


Figure 17: Calculated hydrogen masses in the modeled ITER-FeAT vessels: a) vacuum vessel, b) suppression pool, c) drain tank. Initial phase of accident up to 5,000 seconds.

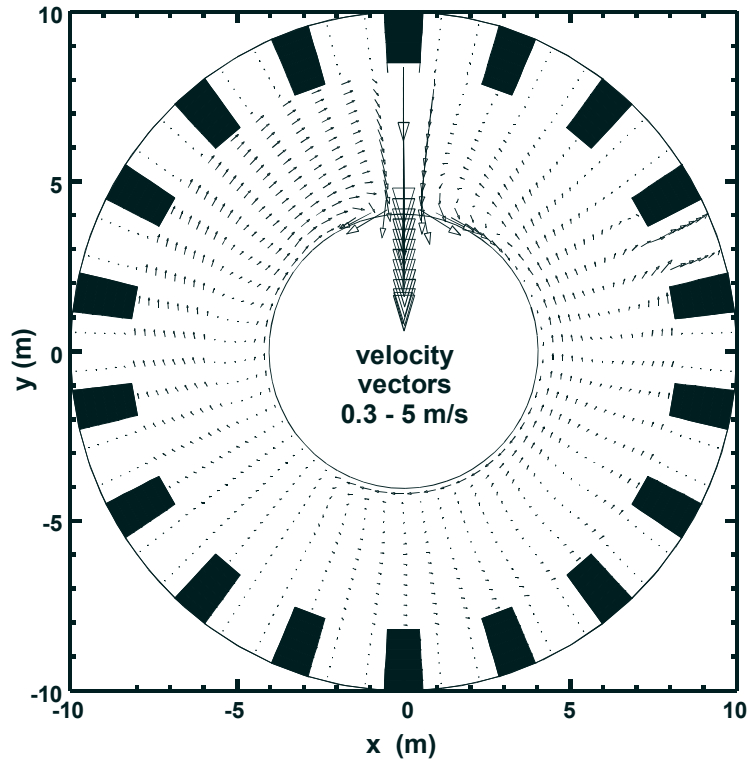


Figure 18: Horizontal cut through the velocity field of the vacuum vessel at the plane of steam injection. Time = 5,000 seconds.

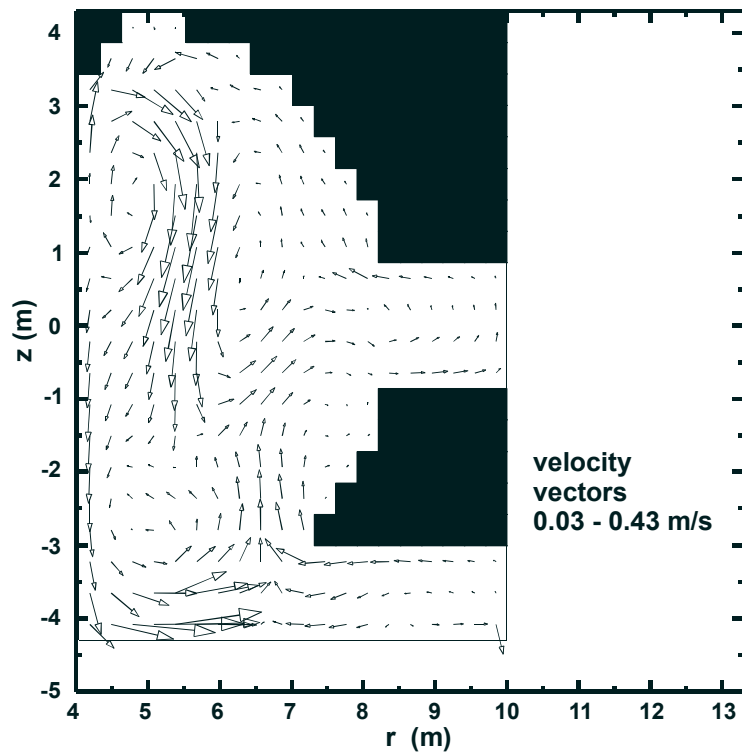


Figure 19: Vertical cut through the velocity field of the vacuum vessel at the position of the pipe leading to the drain tank (in lower right corner of computational domain). Time = 5,000 seconds.

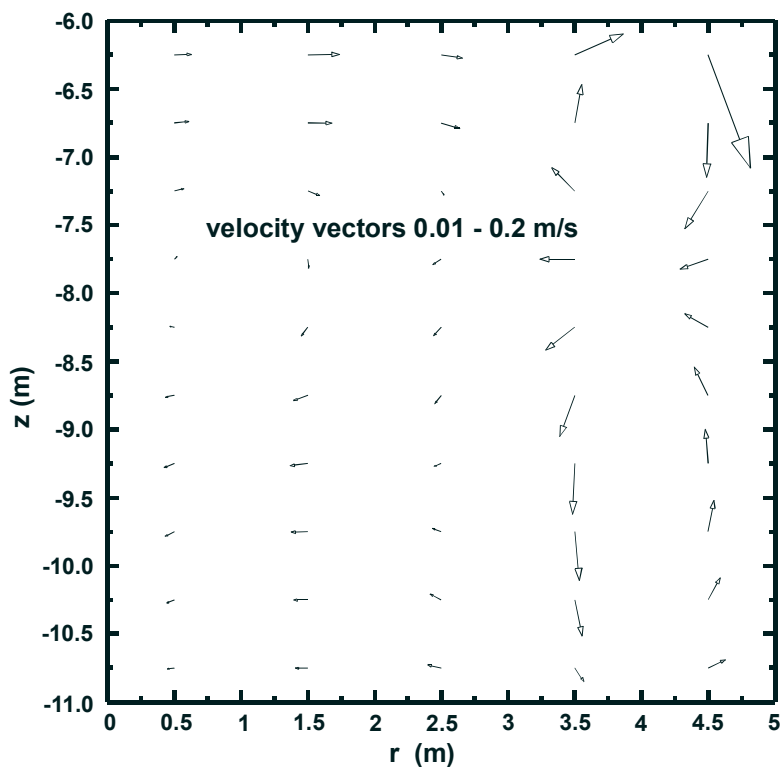


Figure 20: Vertical cut through velocity field of the drain tank at 5,000 seconds.

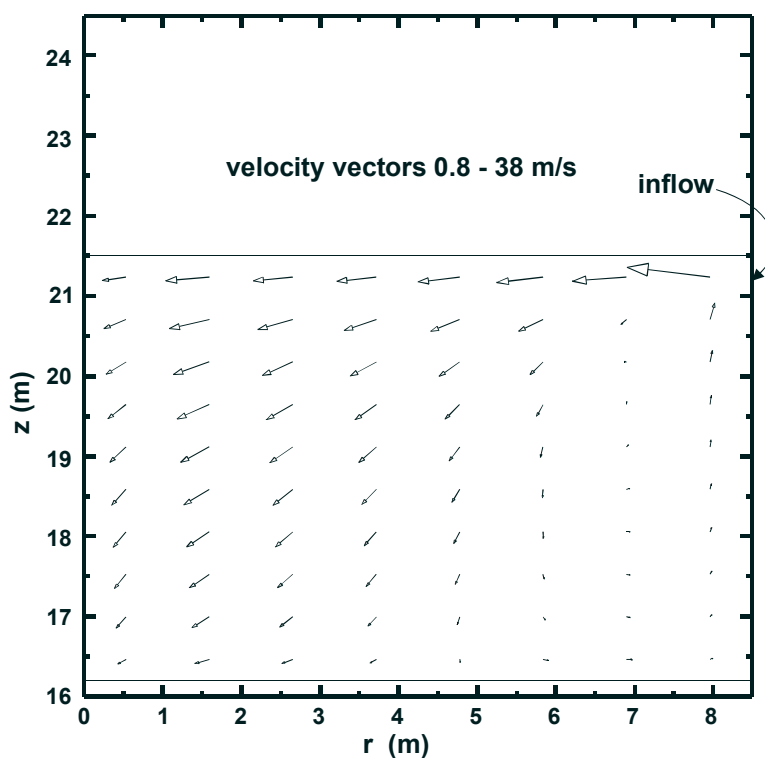


Figure 21: Vertical cut through the velocity field of the cover gas of the pressure suppression system at 5,000 seconds.

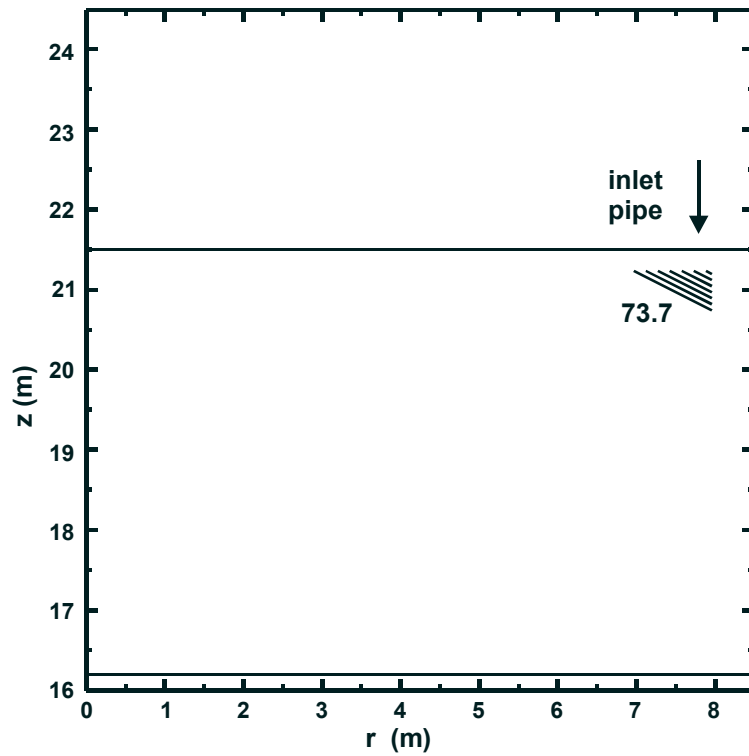


Figure 22: Vertical cut through the suppression pool cover gas, showing the hydrogen concentration field (vol.%) after the end of the hydrogen generation phase (5,000 s, total H<sub>2</sub> inventory 13.8 kg).

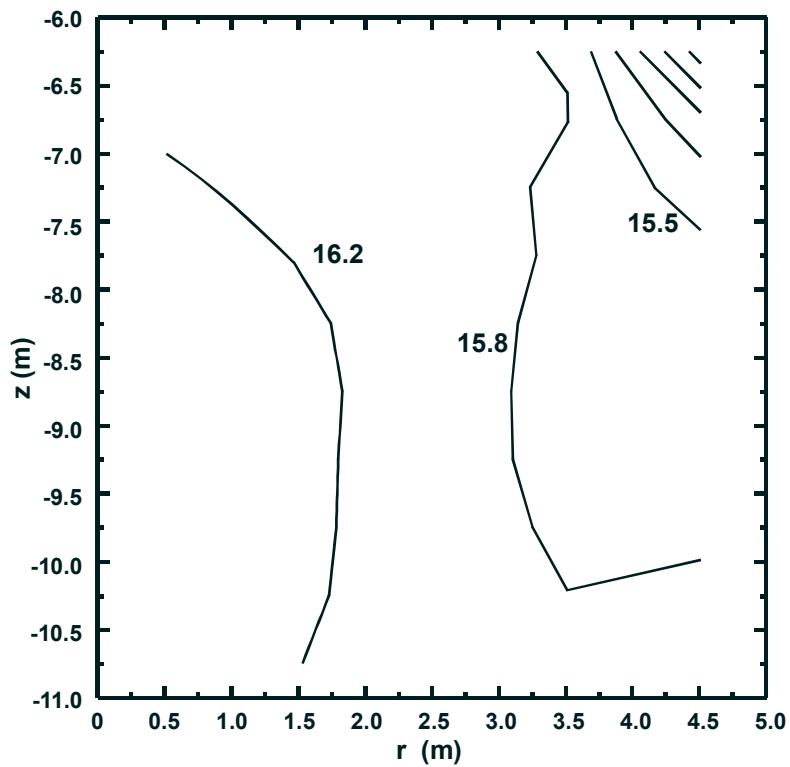


Figure 23: Vertical cut through the hydrogen concentration field (vol.%) in the drain tank after the end of the hydrogen generation phase (5,000 s, total H<sub>2</sub> inventory 0.6 kg).

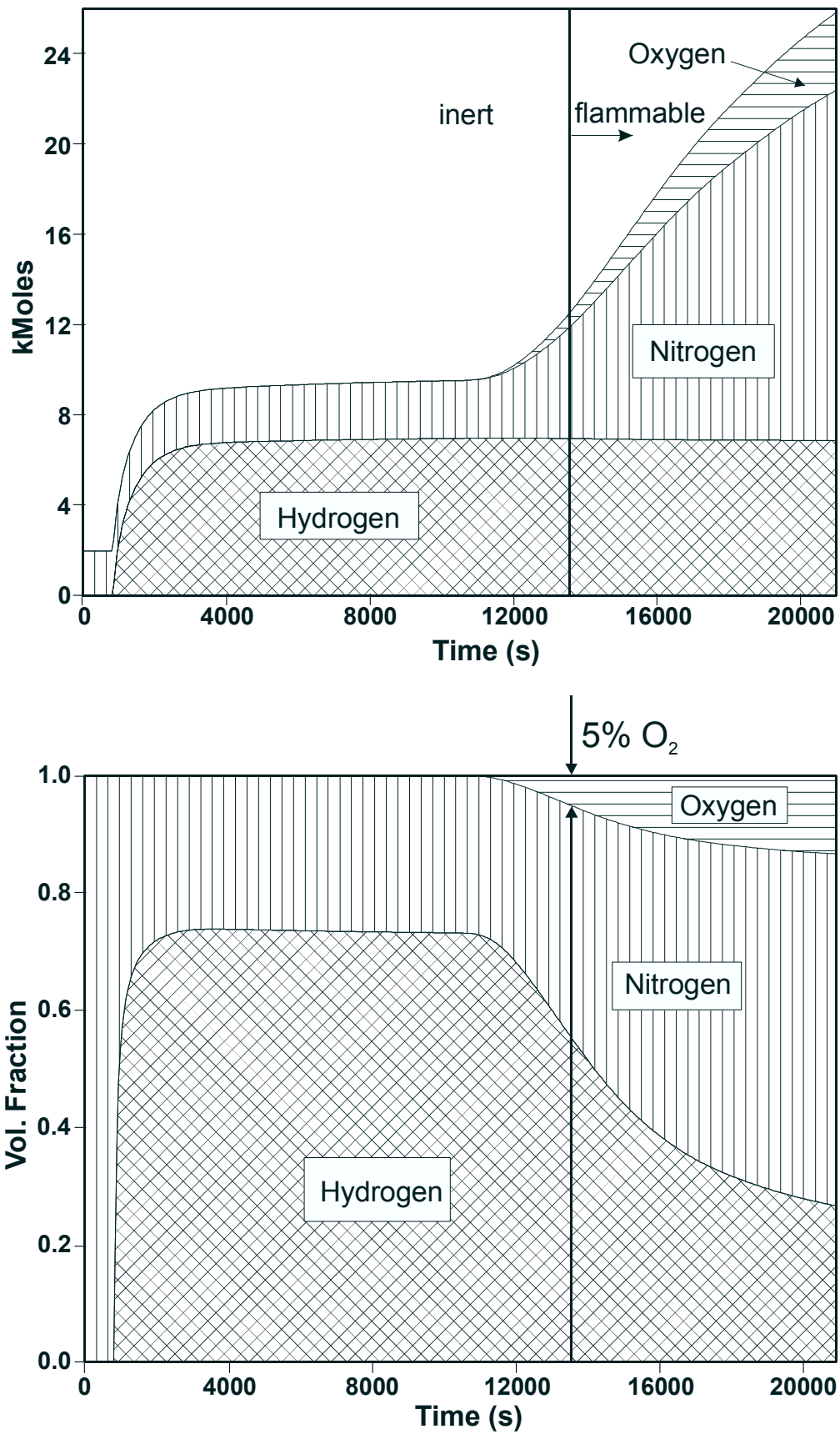


Figure 24: Computed masses and volume fractions of gas components in the suppression pool atmosphere.